A global optimization strategy for the environmentally conscious design of chemical supply chains under uncertainty

Gonzalo Guillén-Gosálbez [a] and Ignacio Grossmann[b] *

[a] *Department of Chemical Engineering, University Rovira i Virgili, Av. Països Catalans, 26, Tarragona, E-43007, Spain*
[b] *Department of Chemical Engineering, Carnegie Mellon University, 5000 Forbes Avenue, Pittsburgh, PA 15213, USA*

Abstract

This paper addresses the optimal design and planning of sustainable chemical supply chains (SCs) in the presence of uncertainty in the damage model used to evaluate their environmental performance. The environmental damage is assessed through the Eco-indicator 99, which includes the recent advances made in Life Cycle Assessment (LCA). The overall problem is formulated as a bi-criterion stochastic non-convex MINLP. The deterministic equivalent of such a model is obtained by reformulating the joint chance constraint employed to calculate the environmental performance of the SC in the space of uncertain parameters. The resulting bi-criterion non-convex MINLP is solved by applying the epsilon constraint method. To guarantee the global optimality of the Pareto solutions found, we propose a novel spatial branch and bound method that exploits the specific structure of the problem. The capabilities of our modeling framework and the performance of the proposed solution strategy are illustrated through a case study.

Key words: Multi-objective optimization, supply chain management, life cycle assessment, uncertainty, global optimization.

1 Introduction

Recently, Guillén-Gosálbez and Grossmann (2008) presented a mathematical formulation to address the environmentally conscious design and planning

* Corresponding author.
Email address: grossmann@cmu.edu (Ignacio Grossmann[b]).

of chemical supply chains. The problem was mathematically formulated as a bi-criterion mixed-integer nonlinear problem (moMINLP) accounting for the maximization of the NPV and minimization of the environmental impact. The environmental performance was measured through the Eco-indicator 99(PRé-Consultants, 2000), which includes the recent advances made in Life Cycle Assessment (LCA). A key issue in this model was the treatment of the uncertainty associated with the life cycle inventory. In this regard, the authors proposed to use a probabilistic constraint to measure the environmental impact of the SC in the space of uncertain parameters. Concepts from chance constrained programming were used to reformulate this constraint into a deterministic equivalent form, and the resulting convex MINLP was solved by a new decomposition strategy based on parametric programming. This approach allowed to decrease the probability of high Eco-indicator 99 values, but did not provide any simultaneous control of the impacts caused in each of its damage categories.

The aim of this paper is to extend the capabilities of the mathematical formulation previously presented by Guillén-Gosálbez and Grossmann (2008) with the aim of dealing with another type of uncertainty that can be encountered in practice, i.e. uncertainty in the parameters of the damage model. An additional objective of this work is to address the simultaneous control of all the damage categories included in the Eco-indicator 99. The core of our new formulation is a joint chance constraint that imposes a probability target of simultaneously satisfying the environmental requirements defined in each impact category. This probabilistic constraint, which replaces the original single chance constraint, leads to a non-convex objective function. To solve the resulting problem to global optimality, we propose a novel spatial branch and bound algorithm that takes advantage of its specific structure. The paper is organized as follows. Section 2 presents a formal definition of the problem under study. In section 3, the mathematical formulation derived to address this problem is presented. Section 4 describes the strategy introduced to solve such a formulation. In section 5 the capabilities of the proposed modeling framework and solution strategy are illustrated through a case study and the conclusions of the work are finally drawn in section 6.

2 Problem statement

Given are a potential network configuration, a fixed time horizon, demand and prices of products in each market and time period, fixed and variable investment costs associated with capacity expansions of plants and warehouses, lower and upper bounds on capacity expansions of plants and warehouses, and costs associated with the SC operation (operating costs of technologies at each manufacturing plant, costs of raw materials, inventory costs at ware-

houses, interest rate, tax rate and salvage value).

The goal is to determine the SC configuration along with the planning decisions that maximize the NPV and minimize the environmental impact. The decisions to be made include:

- Structural decisions: number, location and capacities of plants (including the technologies selected in each of them) and warehouses to be set; transportation links between the SC entities.
- Planning decisions: production rates at the plants in each time period; materials flows between plants, warehouses and markets.

The mathematical formulation derived to address the problem presented above can be found in Guillén-Gosálbez and Grossmann (2008). A brief outline of such a formulation is next given for the sake of completeness of this work.

3 Mathematical formulation

3.1 Mass balances

The mass balances in the manufacturing plants and warehouses are expressed via constraints 1 and 2, and 3, respectively.

$$PU_{jpt} + \sum_{i \in OUT(p)} W_{ijpt} = \sum_{k} Q^{PL}_{jkpt} + \sum_{i \in IN(p)} W_{ijpt} \qquad \forall j, p, t \tag{1}$$

$$W_{ijpt} = \mu_{ip} W_{ijp't} \qquad \forall i, j, p, t \qquad \forall p' \in MP(i) \tag{2}$$

$$INV_{kpt-1} + \sum_{j} Q^{PL}_{jkpt} = \sum_{l} Q^{WH}_{klpt} + INV_{kpt} \qquad \forall k, p, t \tag{3}$$

In these equations PU_{jpt} represents the amount of product p purchased by plant j in period t, W_{ijpt} is the input/output flow of p associated with technology i at plant j in t, Q^{PL}_{jkpt} and Q^{WH}_{klpt} are the flows of p between plant j and warehouse k and warehouse k and market l, respectively, in t, and INV_{kpt} is the inventory of p kept at warehouse k at the end of period t.

Constraints 4 and 6 impose lower and upper limits on the purchases of raw materials (PU_{jpt}) and the sales of products (SA_{lpt}), respectively.

$$\underline{PU_{jpt}} \leq PU_{jpt} \leq \overline{PU_{jpt}} \qquad \forall j, p, t \tag{4}$$

$$\sum_{k} Q^{WH}_{klpt} = SA_{lpt} \qquad \forall l, p, t \tag{5}$$

$$\underline{D_{lpt}^{MK}} \leq SA_{lpt} \leq \overline{D_{lpt}^{MK}} \qquad \forall l, p, t \tag{6}$$

3.2 Capacity constraints

3.2.1 Plants

Equation 7 bounds the capacity expansion in each time period (CE_{ijt}^{PL}), whereas equation 8 defines the total capacity in period t (C_{ijt}^{PL}). Equation 9 limits the number of expansions for technology i available at plant j over the entire planning horizon. Finally, constraint 10 imposes lower and upper production limits based on the existing capacities.

$$\underline{CE_{ijt}^{PL}} X_{ijt}^{PL} \leq CE_{ijt}^{PL} \leq \overline{CE_{ijt}^{PL}} X_{ijt}^{PL} \qquad \forall i, j, t \tag{7}$$

$$C_{ijt}^{PL} = C_{ijt-1}^{PL} + CE_{ijt}^{PL} \qquad \forall i, j, t \tag{8}$$

$$\sum_{t} X_{ijt}^{PL} \leq NEXP_{ij}^{PL} \qquad \forall i, j \tag{9}$$

$$\tau C_{ijt}^{PL} \leq W_{ijpt} \leq C_{ijt}^{PL} \qquad \forall i, j, t \qquad \forall p \in MP(i) \tag{10}$$

3.2.2 Warehouses

Constraints 11, 12 and 13 are equivalent to equations 7, 8 and 9, but apply to warehouses.

$$\underline{CE_{kt}^{WH}} X_{kt}^{WH} \leq CE_{kt}^{WH} \leq \overline{CE_{kt}^{WH}} X_{kt}^{WH} \qquad \forall k, t \tag{11}$$

$$C_{kt}^{WH} = C_{kt-1}^{WH} + CE_{kt}^{WH} \qquad \forall k, t \tag{12}$$

$$\sum_{t} X_{kt}^{WH} \leq NEXP_{k}^{WH} \qquad \forall k \tag{13}$$

In these equations C_{kt}^{WH} and CE_{kt}^{WH} denote the total capacity and capacity expansion of warehouse k in period t, respectively. Equations 14 and 15 impose limits on the inventory kept at each warehouse at the end of period t (INV_{kpt}) and also on the average inventory level (IL_{kt}), which is calculated via equation 16.

$$\sum_{p} INV_{kpt} \leq C_{kt}^{WH} \qquad \forall k, t \tag{14}$$

$$2IL_{kt} \leq C_{kt}^{WH} \qquad \forall k, t \tag{15}$$

$$IL_{kt} = \frac{\sum_{l} \sum_{p} Q_{klpt}^{WH}}{TOR_{k}} \qquad \forall k, t \tag{16}$$

3.2.3 Transportation links

The amount of products sent from plants to warehouses (Q^{PL}_{jkt}) and from warehouses to plants (Q^{WH}_{klt}) must lie between upper and lower limits, provided a transportation link between the corresponding nodes of the network is established, as stated in equations 17 and 18.

$$\underline{Q^{PL}_{jkt}} Y^{PL}_{jkt} \leq Q^{PL}_{jkt} \leq \overline{Q^{PL}_{jkt}} Y^{PL}_{jkt} \qquad \forall j,k,t \tag{17}$$

$$\underline{Q^{WH}_{klt}} Y^{WH}_{klt} \leq Q^{WH}_{klt} \leq \overline{Q^{WH}_{klt}} Y^{WH}_{klt} \qquad \forall k,l,t \tag{18}$$

3.3 Objective function

3.3.1 NPV

Equations 19 to 25 are employed to calculate the NPV, which is determined from the cash flow in each period t (CF_t). This variable is calculated from the net earnings (NE_t), and the fixed investment term in period t($FTDC_t$).

$$NPV = \sum_t \frac{CF_t}{(1+ir)^{t-1}} \tag{19}$$

$$CF_t = NE_t - FTDC_t \qquad t = 1,...,NT-1 \tag{20}$$

$$CF_t = NE_t - FTDC_t + SVFCI \qquad t = NT \tag{21}$$

$$\begin{aligned} NE_t = (1-\varphi) \Bigg[& \sum_l \sum_p \gamma^{FP}_{lpt} SA_{lpt} - \sum_j \sum_p \gamma^{RM}_{jpt} PU_{jpt} \\ & - \sum_i \sum_j \sum_p \upsilon_{ijpt} W_{ijpt} - \sum_k \pi_k IL_{kt} - \sum_j \sum_k \sum_p \psi^{PL}_{jkpt} Q^{PL}_{jkpt} \\ & - \sum_k \sum_l \sum_p \psi^{WH}_{klpt} Q^{WH}_{klpt} \Bigg] + \varphi DEP_t \qquad \forall t \end{aligned} \tag{22}$$

$$DEP_t = \frac{(1-SV)FCI}{NT} \qquad \forall t \tag{23}$$

$$\begin{aligned} FCI = & \sum_i \sum_j \sum_t \left(\alpha^{PL}_{ijt} CE^{PL}_{ijt} + \beta^{PL}_{ijt} X^{P}_{ijt} \right) + \sum_k \sum_t \left(\alpha^{WH}_{kt} CE^{WH}_{kt} + \beta^{WH}_{kt} X^{WH}_{kt} \right) \\ & \sum_j \sum_k \sum_t \left(\beta^{TPL}_{jkt} Y^{PL}_{jkt} \right) + \sum_k \sum_l \sum_t \left(\beta^{TWH}_{klt} Y^{WH}_{klt} \right) \end{aligned} \tag{24}$$

$$FTDC_t = \frac{FCI}{NT} \qquad \forall t \tag{25}$$

Finally, the total amount of capital investment can be constrained to be lower than an upper limit, as stated in equation 26

$$FCI \leq \overline{FCI} \tag{26}$$

3.3.2 Environmental impact

The environmental performance of the network is measured by the Eco-indicator 99. To calculate such a metric, we first compute the life cycle inventory associated with the SC operation (equation 27), which includes the emissions released and feedstock requirements (LCI_b). These entries of the life cycle inventory, which are given by the production of raw materials (PU_{jpt}), the manufacture of final products (W_{ijpt}) and the transport of materials between plants and warehouses (Q^{PL}_{jkpt}) and warehouses and final markets (Q^{WH}_{klpt}), are then translated into a set of damages (DAM_d) caused to the environment (equation 28). In the latter equation, θ_{bc} represents the damage in impact category c per unit of chemical b released to/extracted from the environment.

$$LCI_b = \sum_j \sum_p \sum_t \omega^{PU}_{bp} PU_{jpt} + \sum_i \sum_j \sum_p \sum_t \omega^{PR}_{bp} W_{ijpt} + \sum_i \sum_j \sum_p \sum_t \omega^{EN}_{b} \eta^{EN}_{ijp} W_{ijpt}$$
$$\sum_j \sum_k \sum_p \sum_t \omega^{TR}_{b} \lambda^{PL}_{jk} Q^{PL}_{jkpt} + \sum_k \sum_l \sum_p \sum_t \omega^{TR}_{b} \lambda^{WH}_{kl} Q^{WH}_{klpt} \qquad \forall b \tag{27}$$

$$DAM_d = \sum_{c \in ID(d)} \sum_b \theta_{bc} LCI_b \qquad \forall d \tag{28}$$

The impacts in each damage category (human health, ecosystem quality and resources) are further aggregated into a single metric (i.e., Eco-indicator 99, ECO_{99}) by making using of normalization (δ_d) and weighting factors (ξ_d):

$$ECO_{99} = \sum_d \delta_d \xi_d \cdot DAM_d \tag{29}$$

3.4 Environmental performance under uncertainty: joint chance constraint

In this work, we assume that the life cycle inventory can be perfectly known in advance, whereas the damage factors θ_{bc} are uncertain parameters than can be described through Gaussian probability functions. We should note that the normal probability distribution is one of the most widely used statistical distributions in LCA, and has been repeatedly applied in the literature to characterize different types of uncertainties (Heijungs and Frischknecht, 2005; Heijungs et al., 2005; Sugiyama et al., 2005).

To explicitly control the environmental performance under uncertainty, our

model includes a joint-chance constraint. Such a probabilistic constraint imposes a probability target for simultaneously satisfying the desired environmental requirements in each damage category. This joint chance constraint can be expressed as follows:

$$\Pr\left[\cap DAM_d \leq \Omega_d\right] \geq \kappa \tag{30}$$

In this equation, κ represents a lower limit for the joint probability of not exceeding the individual target levels Ω_d that are defined in each impact category d. The value of κ allows to capture the environmental performance under uncertainty and enters the model as an additional objective to be maximized along with the NPV.

If the damage factors are assumed to be independent (uncorrelated) random variables, then the joint chance constraint can be decomposed into the product of the constituting chance constraints:

$$\prod_d \Pr[DAM_d \leq \Omega_d] \geq \kappa \tag{31}$$

If we now assume that the damage factors follow normal probability distributions, then we can subtract the mean value $\hat{DAM}_d$ and divide by the standard deviation DAM_d^{SD} in order to obtain the corresponding standardized normal distributions in each term of the product:

$$\prod_d \Pr\left[\frac{DAM_d - \hat{DAM}_d}{DAM_d^{SD}} \leq \frac{\Omega_d - \hat{DAM}_d}{DAM_d^{SD}}\right] \geq \kappa \tag{32}$$

$$\prod_d \Phi\left(\frac{\Omega_d - \hat{DAM}_d}{DAM_d^{SD}}\right) \geq \kappa \tag{33}$$

where the mean and standard deviation of the impact caused in each damage category are calculated from the entries of the life cycle inventory and the damage factors as follows:

$$DAM_d^{SD} = \left[\sum_{c \in ID(d)} \sum_b \left(\sigma_{bc}^{DF} LCI_b\right)^2\right]^{1/2} \qquad \forall d \tag{34}$$

$$\hat{DAM}_d = \sum_{c \in ID(d)} \sum_b \hat{\theta_{bc}} LCI_b \qquad \forall d \tag{35}$$

Note that the product on the left-hand side of constraint 33 is neither convex nor concave. However, it is possible to apply a logarithmic transformation in order to express this product as a summation of logarithmic functions:

$$\sum_d \ln \Phi\left(\frac{\Omega_d - \hat{DAM}_d}{DAM_d^{SD}}\right) \geq \ln \kappa \tag{36}$$

The environmental performance under uncertainty, which is defined by equation 36, is finally incorporated into the model. This gives rise to a bi-criterion non-convex MINLP of the following form:

$$\begin{aligned} \text{(P1)} \quad & \max_{x,y} \quad \left(NPV(x,y), \sum_d \ln \Phi \left(\frac{\Omega_d - D\hat{A}M_d}{DAM_d^{SD}} \right) \right) \\ & \text{s.t.} \quad \text{equations 1-27 and 34-35} \end{aligned}$$

Model (P1) can then be solved by any standard algorithm for multi-objective optimization, such as the epsilon constraint or weighted-sum methods, or strategies based on parametric programming. Note that the weighted-sum method is not suitable for our problem, since the Pareto set of (P1) is non-convex due to the presence of binary variables and also to the non-convex nature of the objective function. Furthermore, this non-convexity brought by the calculation of the environmental performance under uncertainty hampers the application of the decomposition strategy based on parametric programming introduced in our previous work (Guillén-Gosálbez and Grossmann, 2008).

Thus, to approximate the Pareto set of (P1) we propose to use the epsilon constraint method (Haimes et al., 1971), which in our case entails the solution of a set of single-objective problems (P2), which are solved for different values of the parameter ϵ:

$$\begin{aligned} \text{(P2)} \quad & \max_{x,y} \quad \sum_d \ln \Phi \left(\frac{\Omega_d - D\hat{A}M_d}{DAM_d^{SD}} \right) \\ & \text{s.t.} \quad NPV(x,y) \leq \epsilon \\ & \qquad \text{equations 1-27 and 34-35} \end{aligned}$$

The objective function in (P2) can be reformulated as follows:

$$\max_{x,y} \quad \sum_d \ln \Phi \left(\frac{A_d}{B_d} \right)$$

where A_d and B_d are two auxiliary continuous variables whose definition is enforced via the following constraints:

$$A_d = \Omega_d - D\hat{A}M_d \qquad \forall d \tag{37}$$

$$\left[\sum_{c \in ID(d)} \sum_b \left(\sigma_{bc}^{DF} LCI_b \right)^2 \right]^{1/2} = B_d \qquad \forall d \tag{38}$$

The left-hand side of equation 38 defines a convex mathematical function, as was shown by Kataoka (1963). Since the equality leads to a non-convex feasible

region, the equation can be relaxed for positive values of A_d as follows:

$$\left[\sum_{c\in ID(d)}\sum_{b}\left(\sigma_{bc}^{DF}LCI_b\right)^2\right]^{1/2} \leq B_d \qquad \forall d \tag{39}$$

The overall problem can therefore be expressed as follows:

$$\begin{array}{lll} \text{(P3)} & \max\limits_{x,y} & \sum_d \ln\Phi\left(\frac{A_d}{B_d}\right) \\ & \text{s.t.} & NPV(x,y) \leq \epsilon \\ & & \text{equations 1-27, 35,37 and 39} \end{array}$$

In this formulation, the lower and upper limits that define the interval within which the epsilon parameter must fall (i.e, $\epsilon \in [\underline{\epsilon}, \overline{\epsilon}]$), can be obtained by solving each objective separately:

$$\begin{array}{lllll} \text{(P3a)} & (x^*, y^*) = & \arg\max\limits_{x,y} & \sum_d \ln\Phi\left(\frac{A_d}{B_d}\right) \\ & & \text{s.t.} & \text{equations 1-27, 35,37 and 39} \end{array}$$

which defines $\underline{\epsilon} = NPV(x^*, y^*)$ and

$$\begin{array}{lllll} \text{(P3b)} & (x^*, y^*) = & \arg\max\limits_{x,y} & NPV(x,y) \\ & & \text{s.t.} & \text{equations 1-27, 35,37 and 39} \end{array}$$

which defines $\overline{\epsilon} = NPV(x^*, y^*)$.

With the transformations presented before, (P2) has been reformulated into a model (P3) with a non-convex objective function subject to a set of convex constraints that define a convex feasible region. We next present a method to solve (P3) to global optimality that exploits its specific mathematical structure.

4 Solution procedure

We describe in this section an optimization method to solve to global optimality any instance of problem (P3), which will be denoted from now on as follows:

$$
\begin{array}{lll}
\text{(P4)} \quad \max\limits_{x,y} & \sum_d \ln \Phi\left(\frac{A_d}{B_d}\right) & \\
\text{s.t.} & h_j(x,y) = 0 & j = 1, ...J \\
& g_l(x,y) \leq 0 & l = 1, ...L \\
& x \in \Re^n \, , \, y \in \{0,1\}^m &
\end{array}
$$

where the equality constraints $h_j(x,y)$ are all linear, and the inequalities $g_l(x,y)$ are all linear except constraint 39, which is nonlinear but convex.

Our solution method relies on some properties of (P4) that are formalized in the propositions given bellow. The proofs of these propositions can be found in the Appendix.

Proposition 1. *Consider the multi-objective problem:*

$$
\begin{array}{lll}
\text{(P5)} \quad \max\limits_{x,y} & \left(\ln \Phi\left(\frac{A_1}{B_1}\right), ..., \ln \Phi\left(\frac{A_D}{B_D}\right)\right) & \\
\text{s.t.} & h_j(x,y) = 0 & j = 1, ...J \\
& g_l(x,y) \leq 0 & l = 1, ...L \\
& x \in \Re^n \, , \, y \in \{0,1\}^m &
\end{array}
$$

Let $(\hat{x}, \hat{y})$ be a global maximum of (P4). Then $(\hat{x}, \hat{y})$ is a Pareto solution of (P5).

The global maximum of (P4) is a Pareto solution of (P5), and therefore can be generated by the epsilon constraint method. The application of such a method to (P5) entails the solution of different instances of (P6), each of which is calculated for a specific set of values of the auxiliary epsilon parameters ϵ_d:

$$
\begin{array}{lll}
\text{(P6)} \quad \max\limits_{x,y} & \ln \Phi\left(\frac{A_k}{B_k}\right) & \\
\text{s.t.} & \ln \Phi\left(\frac{A_d}{B_d}\right) \geq \epsilon_d & d \neq k \\
& h_j(x,y) = 0 & j = 1, ...J \\
& g_l(x,y) \leq 0 & l = 1, ...L \\
& x \in \Re^n \, , \, y \in \{0,1\}^m &
\end{array}
$$

In this formulation, ϵ_d denotes the targets imposed to the terms of the objective function that are transferred to some constraints. Problem (P6) has a useful property that is formally stated in the following proposition.

Proposition 2. *Any point satisfying the Karush-Kuhn-Tucker conditions of (P6) is a global maximum of (P6).*

Our method also exploits another mathematical property satisfied by a global maximum of (P4), which is given in the next proposition.

Proposition 3. *Let $(\hat{x}, \hat{y})$ satisfy the Karush-Kuhn-Tucker conditions of (P4). Then $(\hat{x}, \hat{y})$ is a Pareto solution of (P5) that satisfies the following condition:*

$$\left(\frac{\partial \ln \Phi\left(\frac{A_k}{B_k}\right)}{\partial \ln \Phi\left(\frac{A_d}{B_d}\right)}\right)_{\left(\delta \ln \Phi\left(\frac{A_i}{B_i}\right)=0,\, i\neq d,k\right)\wedge(\delta g_l(x,y)=0)} = -1 \qquad d \neq k \tag{40}$$

Figure 1 illustrates the idea behind Propositions 1 and 3 for a problem with two terms in the objective function. The top of the figure depicts the objective function of the problem in the space of the original set of decision variables. In the bottom of the Figure, the Pareto curve that trades-off the terms of the objective function is given. In this example, the model has two different local optima, one of which is in turn a global optimum. As can be observed in the figure, the global optimum of (P4) belongs to the Pareto set that trades-off the terms of its objective function. Furthermore, it can be observed how the local maxima are the intersection points of the line $\ln \Phi(\frac{A_1}{B_1}) + \ln \Phi(\frac{A_2}{B_2}) = c$, with the feasible region of (P5), where the value of c is the local maximum value that makes this intersection non-empty. In these local solutions, the KKT conditions of (P4) are satisfied and we also have:

$$\left(\frac{\partial \ln \Phi(\frac{A_1}{B_1})}{\partial \ln \Phi\left(\frac{A_2}{B_2}\right)}\right) = \left(\frac{\partial \ln \Phi\left(\frac{A_2}{B_2}\right)}{\partial \ln \Phi\left(\frac{A_1}{B_1}\right)}\right) = -1$$

In general, model (P4) may have several KKT points, so the problem consists of identifying the one that corresponds to a global optimum of (P4). These theoretical insights into (P4) suggest a possible solution procedure that consists of calculating the Pareto set of (P5) and then picking the Pareto solution for which the summation of the terms of the original objective function is maximum.

As mentioned above, the global maximum of (P4) can be obtained by generating the Pareto set of (P5). Furthermore, if (P5) is solved by the epsilon constraint method, then from Proposition 2 we know that a local optimum of any instance of (P6) is also a global optimum.

In fact, there is more efficient way of conducting the search of a global optimum of (P4) by making use of a spatial branch and bound framework (see Figure 2). The underlying idea consists of partitioning the feasible space into smaller domains, each of which corresponds to a node of the branch and bound tree, in which valid lower and upper bounds on the value of the objective function are obtained. The partition of the feasible region is carried out by choosing a term k of the objective function, which will be regarded as main objective, and

then branching on the values of the remaining $|D|-1$ terms. Thus, at each node i, valid lower bounds are calculated by locally optimizing the following single objective problem:

$$\begin{array}{lll} \max\limits_{x,y} & \sum_d \ln \Phi\left(\frac{A_d}{B_d}\right) & \\ \text{s.t.} & \underline{\epsilon_d^i} \leq \ln \Phi\left(\frac{A_p}{B_p}\right) \leq \overline{\epsilon_d^i} & d \neq k \\ & h_j(x,y) = 0 & j = 1, ...J \\ & g_l(x,y) \leq 0 & l = 1, ...L \\ & x \in \Re^n \, , \, y \in \{0,1\}^m & \end{array} \tag{P7}$$

where $\underline{\epsilon_d^i}$ and $\overline{\epsilon_d^i}$ denote the lower and upper limits imposed to the term d of the objective function in each node i of the tree, and k represents the term of the objective function that is regarded as main objective. Valid upper bounds on the objective function value can also be obtained by making use of the following proposition:

Proposition 4. *A valid upper bound to problem (P7) at node i is given by the following expression*

$$UB^i = UB_k^i + \sum_{d \neq k} \overline{\epsilon_d^i} \tag{41}$$

where UB_k denotes the value of a global optimal solution of the following problem:

$$\begin{array}{llll} UB_k^i = & \max\limits_{x,y} & \ln \Phi\left(\frac{A_k}{B_k}\right) & \\ & \text{s.t.} & \ln \Phi\left(\frac{A_d}{B_d}\right) \geq \underline{\epsilon_d^i} & d \neq k \\ & & h_j(x,y) = 0 & j = 1, ...J \\ & & g_l(x,y) \leq 0 & l = 1, ...L \\ & & x \in \Re^n \, , \, y \in \{0,1\}^m & \end{array} \tag{P8}$$

Note that from Proposition 2, any KKT point of (P8) is a global maximum of (P8).

4.1 Algorithmic steps

The outline of the proposed global optimization algorithm is as follows:

- **Step 0** (initialization). Set the following values: number of nodes, $i = 1$; overall lower bound, $OLB = -\infty$; overall upper bound, $OUB = \infty$. Com-

pute for every d the lower and upper limits $\underline{\epsilon_d^i}$ and $\overline{\epsilon_d^i}$ that define the intervals $[\underline{\epsilon_d^i}, \overline{\epsilon_d^i}]$ within which the terms of the objective function must fall as follows:

$$\begin{aligned} \text{(P9)} \quad \overline{\epsilon_d^i} = \max_{x,y} \quad & \ln \Phi \left(\tfrac{A_d}{B_d}\right) \\ \text{s.t.} \quad & h_j(x,y) = 0 \qquad j = 1, ...J \\ & g_l(x,y) \leq 0 \qquad l = 1, ...L \\ & x \in \Re^n \, , \, y \in \{0,1\}^m \end{aligned}$$

$$\underline{\epsilon_d^i} = \min_d \left(f_d(\hat{x_d}, \hat{y_d})\right)$$

where $(\hat{x_d}, \hat{y_d})$ denotes the optimal solution of (P9), and $f_d(\hat{x_d}, \hat{y_d})$ is the value of the term d of the objective function associated with such a solution. Identify the k term of the objective function for which the difference $\overline{\epsilon_d^i} - \underline{\epsilon_d^i}$ is maximum. This term will be regarded as the main objective.

- **Step 1** (lower bound). Obtain a lower bound (LB_i) of (P4) in node i by locally optimizing ($P7$) in the search space defined by the intervals $[\underline{\epsilon_d^i}, \overline{\epsilon_d^i}]$. Update the overall lower bound (OLB) whenever an improvement takes place.
- **Step 2** (upper bound). Obtain an upper bound (UB_i) of (P4) in node i by making use of Proposition 4. The overall upper bound (OUB) must be updated in each iteration.
- **Step 3** (convergence). A node can be discarded from the tree if the upper bound at that node is lower than the current best lower bound OLB, or if it is within a tolerance tol of OLB. Thus, those nodes i for which the relaxation gap (gap_i) is less than tol, are fathomed. The relaxation gap is defined as:

$$gap_i = |\frac{OLB - UB_i}{OLB}| \tag{42}$$

  The search is stopped when no open nodes are left in the tree.
- **Step 4** (spatial branch and bound). Select a node n for which the relaxation gap gap_n is greater than the specified tolerance. Branch down this node according to some rules in order to create two child nodes. This is done by partitioning the search space of the original node, which is defined by the intervals $[\underline{\epsilon_d^n}, \overline{\epsilon_d^n}]$, into two disjoint sub-regions, each of which corresponds to the sub-intervals $[\underline{\epsilon_d^{n+1}}, \overline{\epsilon_d^{n+1}}]$ and $[\underline{\epsilon_d^{n+2}}, \overline{\epsilon_d^{n+2}}]$, respectively. Update the number of nodes (i.e., $i = i + 2$) and then repeat steps 1 to 4 for each of the new nodes.

It is important to highlight the following points of the algorithm:

(1) The method presented in this paper can be applied to any minimization/maximization problem where the objective function can be expressed

as a summation of pseudoconvex/pseudoconcave or strictly quasiconvex/quasiconcave functions over a convex feasible region.

(2) The proposed strategy does not make use of convex envelopes to calculate valid upper bounds for the problem. The computation of these bounds is carried out by solving problem (P8) in each node of the tree, for which any KKT point is a global maximum.

(3) Problem (P7) can be expressed as follows:

$$\begin{array}{lll} \text{(P7')} \quad \max\limits_{x,y} & \sum_d \ln \Phi(\frac{A_d}{B_d}) & \\ \text{s.t.} & -A_d + \Phi^{-1}(e^{\frac{\epsilon_d^i}{-}})B_d \leq 0 & d \neq k \\ & A_d - \Phi^{-1}(e^{\overline{\epsilon_d^i}})B_d \leq 0 & d \neq k \\ & h_j(x,y) = 0 & j = 1, ...J \\ & g_l(x,y) \leq 0 & l = 1, ...L \\ & x \in \Re^n \, , \, y \in \{0,1\}^m & \end{array}$$

where the nonlinear epsilon constraints have been reformulated into a linear form. Furthermore, problem (P8) can also be reformulated into the following form:

$$\begin{array}{llll} \text{(P8')} \quad UB_k^i = & \max\limits_{x,y} & \frac{A_k}{B_k} & \\ & \text{s.t.} & -A_d + \Phi^{-1}(e^{\frac{\epsilon_d^i}{-}})B_d \leq 0 & d \neq k \\ & & h_j(x,y) = 0 & j = 1, ...J \\ & & g_l(x,y) \leq 0 & l = 1, ...L \\ & & x \in \Re^n \, , \, y \in \{0,1\}^m & \end{array}$$

since the function $\ln \Phi(\cdot)$ is monotone increasing. These reformulations reduce the number of non-linearities and improve the robustness of the NLP subproblems.

(4) The optimality gap should be expressed in the domain of the original joint probability (i.e., $\prod_d \Phi(\cdot)$) associated with the best solution found so far and the best possible solution. This leads to lower optimality gaps and more efficient of the algorithm.

(5) One of the child nodes generated after branching down a parent node will inherit the value of UB_k^i from the parent node. Thus, the upper bounding problem (P8) has to be solved in half of the nodes of the tree. This is illustrated in Figure 3. Notice that the calculation of valid upper bounds for the parent node and its child nodes entails solving the same instance of (P8). Furthermore, since no upper limits are imposed on the terms of the objective function, it may also happen that both child nodes will inherit the value of UB_k^i from the parent node. This will lead to a decrease in the total number of upper bounding problems to be solved, and therefore to a reduction in the CPU time required by the algorithm.

(6) The lower bounding problem is only solved after calculating the upper

bound and checking the convergence criteria in the node. This expedites the search, since those nodes of the tree for which the solution of the upper bounding problem (i.e., UB_k^i) is given by the parent node will be quickly fathomed if they do not satisfy the convergence criteria. This avoids having to solve a large number of lower bounding problems in the entire tree.

(7) The upper and lower bounds calculated through the estimator equations are updated in each child node, so we obtain tighter bounds in each of the sub-regions.

(8) Certain heuristics are followed to branch on the terms of the objective function. Specifically, in each node we branch on the term d of the objective function for which the difference dif_d between the upper and lower limits that define the search space (i.e., $dif_d = \overline{\epsilon_d^i} - \underline{\epsilon_d^i}$) is maximum. Furthermore, we select the mid-point of the limits of the term d as the branching point (bisection rule). A depth first strategy is used to explore the nodes of the tree.

(9) Theoretically, the spatial branch and bound is an infinite process since the branching is done on the continuous variables, but terminates in a finite number of nodes when we apply the convergence criteria for the desired non-zero tolerance tol.

(10) Our method can only generate Pareto solutions for which the probability of satisfying each target level is at least 50 %. This is due to the reformulation made in equation 38, which preserves the convexity of the model by forcing the numerator inside the normal function to take positive values. This however is not a major limitation since one is only normally interested in those Pareto solutions that have large probabilities of satisfying the target levels. Furthermore, the maximum NPV solution, which does not necessarily have to satisfy the above posed requirement, can be computed by solving an MILP, in which the NPV is regarded as main objective, and the nonlinear equations that define the joint chance constraint are dropped.

5 Case study

We next consider two variants of the first example introduced by Guillén-Gosálbez and Grossmann (2008) to illustrate the application and computational effectiveness of the proposed algorithm. These new examples only differ in the transportation costs, which play a major role in the design problem.

The models were implemented in GAMS 21.4 (Brooke et al., 1998), and solved with the MINLP solver SBB using CONOPT 3 on an Intel 1.2 GHz machine. Note that the nonlinear branch and bound method implemented in SBB guarantees the global optimality of the solutions found. This is due to the fact that

CONOPT solves the NLPs of the nodes of the tree to global optimality (see Proposition 2). We should also remark that DICOPT does not exhibit this property and therefore has not been used, since the supporting hyper-planes employed by the outer approximation method are only valid for convex problems, which is not our case. Finally, a direct comparison between our strategy and BARON, the state of the art software for global optimization, was not possible, since BARON cannot handle the error function that appears in the objective function of our model.

5.1 Case study 1A

This problem addresses the optimal retrofit of an existing SC established in Europe in terms of economic and environmental performance under uncertainty. The superstructure of the case study is depicted in Figure 4, whereas the set of available technologies is given in Figure 5. Specifically, there are 6 different technologies available to manufacture six main products: acetaldehyde, acetone, acrylonitrile, cumene, isopropanol and phenol. The original SC comprises 1 plant and 1 warehouse that are both placed in Tarragona (Spain), and 4 final markets that are located in the following European cities: Leuna (Germany), Neratovice (Czech Republic), Sines (Portugal) and Tarragona. The demand is expected to increase in Leuna and Neratovice, so the problem consists of determining whether it is better to expand the capacity of the existing plant or open a new one in Neratovice, which would be close to the growing markets.

A demand satisfaction target level of 40 % must be attained in each of the years of a 3-year time horizon. The existing plant has an installed capacity of 100 kton/year for each available technology, whereas the capacity of the existing warehouse equals 100 kton. No limits on the total number of expansions of plants and warehouses are imposed. The lower and upper bounds for the capacity expansions at plants and warehouses are 10 and 400 kton/year for the plants, and 5 and 400 ktons for the warehouses, respectively.

No upper limits on the purchases of raw materials are specified. On the other hand, to prevent outsourcing from taking place, we set zero upper limits on the purchases of intermediate and final products. The lower and upper bounds on the flows of materials between plants and warehouses, and warehouses and markets are 5 and 500 kton/year in both cases, respectively. The turnover ratio is equal to 10 and the initial inventories at the warehouses are assumed to be zero. No minimum production levels are fixed at the plants. The interest rate, the salvage value and the tax rate are equal to 10%, 20% and 30%, respectively. In this first example, we assume low transportation costs equal to 1.7 ¢/ton $\cdot$ km. The fixed investment terms associated with the establishment

of transportation links are all set to zero. All the remaining data associated with the problem is given in Tables 1 to 7.

The entries of the life cycle inventory of our example are taken from different databases that are integrated within the Simapro software (PRé-Consultants, 1998). The direct emissions associated with the manufacturing technologies are neglected. With regard to the description of the uncertainty that affects the damage model, we assume standard deviations of 10 % in all the damage factors that fall in the human health impact category, except for the damage caused by climate change, for which a 30 % value is considered. On the other hand, the standard deviations considered in the impacts that belong to the ecosystem quality and resources categories are 20 and 25 %, respectively. The mean values of the damage factors are all taken from the literature (PRé-Consultants, 2000). The environmental targets that should not be exceeded in each impact category are 4.5 $\cdot 10^3$ DALYs for the human health, 3.3 $\cdot 10^8$ PDF$\cdot$m$^2\cdot$year for the ecosystem quality and 1.2 $\cdot 10^{10}$ MJ for the resources.

The values of $\underline{\epsilon}$ and $\bar{\epsilon}$ that define the interval within which the NPV of the problem must fall are firstly calculated by maximizing both objectives separately. The interval $[\underline{\epsilon}, \bar{\epsilon}]$ is next partitioned into 20 subintervals of equal length, and model (P3) is then calculated for every possible value of ϵ. Each instance of (P3) is solved to global optimality with an optimality gap (i.e., tolerance) of 0.1 %. The model has 1,963 constraints, 1,837 continuous variables and 78 binary variables. The total CPU time that was required is 1,127.55 CPU seconds.

Figure 6 shows the Pareto solutions obtained by following the proposed procedure. Each point of the Pareto set entails a specific SC structure and a set of planning decisions. As can be observed, there is a clear trade-off between the NPV and the environmental impact.

Note that the Pareto solutions given in Figure 6 are those for which the probabilities of satisfying each individual target level are at least 50 %. The most profitable solution of this example does not satisfy this condition, and therefore is computed by an additional MILP, as described before. Such a solution leads to a NPV of $ 157 millions, which is 45 % higher than the one obtained by the minimum environmental impact solution ($ 157 millions vs. $ 108 millions).

Figures 7 and 8 show the SC configurations of the extreme solutions (the maximum NPV and minimum environmental impact alternatives). The figures in the plot represent the capacities of the plants and warehouses expressed in tons per year and tons, respectively. As can be observed, both solutions entail the construction of a new plant in Neratovice. However, they primarily differ in the SC topology and the total network capacity. In the maximum NPV solution, part of the total production is made in the new plant that will be

opened in Neratovice, and then shipped to the warehouse that is close to the existing plant. By doing so, the model takes advantage of the lower investment and production costs in Czech Republic compared to Spain. On the other hand, in the minimum environmental impact solution, products are manufactured as close as possible to the markets. This SC topology reduces the emissions due to the transportation tasks. The second difference lies in the SC capacity, which is lower in the minimum environmental impact design. In this solution, the production rates are reduced and the demand satisfaction level drops to its lower limit which was set to 40 %.

Figures 9 to 11 depict the probability curves associated with the maximum NPV and minimum environmental impact solutions, respectively. As can be observed, when the joint probability is increased, the probability curves are all shifted to the left, thus providing a simultaneous control of all the impact categories in the space of uncertain parameters.

Figure 12 depicts for each of the extreme solutions, the expected environmental impacts in all the damage categories covered by the Eco-indicator 99. In both cases, the main impacts are: (3) respiratory effects on humans caused by inorganic substances, (4) damage to human health caused by climate change and (11) damage to resources caused by extraction of fossil fuels. Finally, Figures 13 and 14 show the contribution of the different sources of impact to the total environmental damage. Note that in all the cases the generation of raw materials represents the most significant contribution to the total impact.

5.2 Case study 1B

In the former case study, the extreme solutions of the Pareto set led to different SC topologies. This was motivated by the low transportation costs, as was commented before. In this new example, the materials flows between the SC entities are penalized with higher transportation costs (i.e., 21 ¢/ ton $\cdot$ km). The goal is to investigate the impact that this cost has in the topological features of the extreme solutions of the Pareto set, assuming that the remaining data of the problem are kept constant.

We compute 20 Pareto points with an optimality gap of 0.1 % by following the same strategy as before. The total CPU time required is 213.94 s. Figure 15 shows the Pareto solutions of the problem. As can be observed, the higher transportation costs make the NPV drop about 15 % on average. As a result, the entire Pareto set is moved to the left. As occurred in the previous case, an additional MILP is required to calculate the most profitable alternative. This solution yields an NPV of $ 124 millions, whereas the minimum environmental impact alternative leads to $ 90 millions.

The extreme configurations of the Pareto set are given in Figures 16 and 17, along with the capacities of the plants and warehouses. As opposed to the previous case, in this example the extreme solutions lead to the same topology and only differ in the total network capacity, which is lower in the minimum environmental impact solution. Thus, both solutions seek to reduce the transportation flows, since this policy simultaneously results in lower total costs and environmental impacts.

The probability curves associated with the aforementioned solutions are shown in Figures 18 to 20. Comparing the probability curves of the maximum NPV solutions obtained in both examples, one can notice that in the second case they have been moved to the left. This is due to the higher transportation costs, which have forced the model to reduce the materials flows and therefore the emissions generated by the transportation tasks. On the other hand, the minimum environmental impact curves are similar in both cases.

6 Conclusions

This paper has addressed the optimal design and planning of sustainable chemical processes with environmental concerns. The environmental impact associated with the SC operation has been assessed through the Eco-indicator 99, which includes recent advances made in LCA. The uncertainty of the damage model that translates the life cycle inventory into impacts caused to the environment has been explicitly incorporated into our formulation.

The overall problem has been formulated as a bi-criterion chance constrained MINLP. Two objectives has been considered in such a formulation: (1) the NPV and (2) the joint probability of simultaneously satisfying all the environmental targets defined in each damage category of the Eco-indicator 99. The deterministic equivalent of this model has been derived by reformulating the joint chance constraint that defines the environmental performance under uncertainty. The resulting bi-criterion non-convex MINLP has been solved by applying the epsilon constraint method. To guarantee the global optimality of the Pareto solutions, we have introduced a novel branch and bound strategy that exploits the mathematical structure of the model.

The performance of our modeling framework and solution strategy have been illustrated through two examples of a case study. Our tool provides a simultaneous control of the impacts caused in the damage categories covered by the Eco-indicator 99. The SC design and planning decisions calculated by the model, which represent the optimal compromise between NPV and environmental performance, aim at facilitating the decision-making process in the area of sustainable chemical process design.

7 Notation

Indices

b	environmental burdens
c	impact categories
d	damage categories
i	manufacturing technologies
j	plants
k	warehouses
l	markets
p	products
t	time periods

Sets

$ID(d)$	set of impacts c contributing to damage category d
$IN(p)$	set of manufacturing technologies that consume p
$MP(i)$	set of main products p of technology i
$OUT(p)$	set of manufacturing technologies that produce p

Parameters

$\overline{CE_{ijt}^{PL}}$	upper bound on the capacity expansion of manufacturing technology i at plant j in time period t
$\underline{CE_{ijt}^{PL}}$	lower bound on the capacity expansion of manufacturing technology i at plant j in time period t
$\overline{CE_{kt}^{WH}}$	upper bound on the capacity expansion of warehouse k in time period t
$\underline{CE_{kt}^{WH}}$	lower bound on the capacity expansion of warehouse k in time period t
$\overline{D_{lpt}^{MK}}$	maximum demand of product p sold at market l in period t
$\underline{D_{lpt}^{MK}}$	minimum demand of product p to be satisfied at market l in period t
ir	interest rate
$\overline{FCI}$	upper limit on the total capital investment
$NEXP_{ij}^{PL}$	maximum number of capacity expansions for technology i available at plant j

$NEXP_k^{WH}$	maximum number of capacity expansions for warehouse k
NT	number of time periods
$\overline{PU_{jpt}}$	upper bound on the purchases of product p at plant j in period t
$\underline{PU_{jpt}}$	lower bound on the purchases of product p at plant j in period t
$\overline{Q_{jkt}^{PL}}$	upper bound on the flow of materials between plant j and warehouse k in time period t
$\underline{Q_{jkt}^{PL}}$	lower bound on the flow of materials between plant j and warehouse k in time period t
$\overline{Q_{klt}^{WH}}$	upper bound on the flow of materials between warehouse k and market l in time period t
$\underline{Q_{klt}^{WH}}$	lower bound on the flow of materials between warehouse k and market l in time period t
SV	salvage value
TOR_k	turnover ratio of warehouse k
μ_{ip}	mass balance coefficient associated with product p and manufacturing technology i
φ	tax rate
γ_{lpt}^{FP}	price of final product p sold at market l in time period t
γ_{jpt}^{RM}	price of raw material p purchased at plant j in time period t
υ_{ijpt}	operating cost of manufacturing technology i available at plant j per unit of main product p in time period t
π_{kt}	inventory cost at warehouse k in period t
ψ_{jkpt}^{PL}	unitary transport cost of product p sent from plant j to warehouse k in time period t
ψ_{klpt}^{WH}	unitary transport cost of product p sent from warehouse k to market l in time period t
α_{ijt}^{PL}	variable investment term associated with technology i at plant j in time period t
α_{kt}^{WH}	variable investment term associated with warehouse k in time period t
β_{ijt}^{PL}	fixed investment term associated with technology i at plant j in time period t

β_{kt}^{WH}	fixed investment term associated with warehouse k in time period t
β_{jkt}^{TPL}	fixed investment term associated with the establishment of a transport link between plant j and warehouse k in time period t
β_{klt}^{TWH}	fixed investment term associated with the establishment of a transport link between warehouse k and market l in time period t
ω_{bp}^{PU}	emissisions/feedstock requirements of chemical b per unit of raw material p generated
ω_{bp}^{PR}	emissisions/feedstock requirements of chemical b per unit of intermediate/final product p generated
ω_{b}^{EN}	emissisions/feedstock requirements of chemical b per unit of FOET combusted
ω_{b}^{TR}	emissisions/feedstock requirements of chemical b per unit of mass transported one unit of distance
η_{ijp}^{EN}	energy consumed per unit of chemical p produced with manufacturing technology i at plant j
λ_{jk}^{PL}	distance between plant j and warehouse k
λ_{kl}^{WH}	distance between warehouse k and market l
θ_{bc}	damage factor of chemical b contributing to impact category c
$\hat{\theta_{bc}}$	mean value of damage factor of chemical b contributing to impact category c
σ_{bc}^{DF}	standard deviation of damage factor of chemical b contributing to impact category c
Ω_d	Target level for damage category d
κ	joint probability of not exceeding the individual target levels Ω_d)
δ_d	normalization factor for damage category d
ξ_d	weighting factor for damage category d
τ	minimum desired percentage of the available installed capacity that must be utilized

Variables

C_{ijt}^{PL}	capacity of manufacturing technology i at plant j in time period t

CE_{ijt}^{PL}	capacity expansion of manufacturing technology i at plant j in time period t
C_{kt}^{WH}	capacity of warehouse k in time period t
CE_{kt}^{WH}	capacity expansion of warehouse k in time period t
CF_t	cash flow in period t
DAM_d	impact in damage category d
$D\hat{A}M_d$	mean value of impact in damage category d
DAM_d^{SD}	standard deviation of impact in damage category d
DEP_t	depreciation term in period t
ECO_{99}	Eco-indicator 99
FCI	fixed capital investment
$FTDC_t$	fraction of the total depreciable capital that must be paid in period t
IL_{kt}	average inventory level at warehouse k in time period t
IM_c	damage in impact category c
INV_{kpt}	inventory of product p kept at warehouse k in period t
LCI_b	life cycle inventory entry (i.e., emissisions/feedstock requirements) associated with chemical b
NE_t	net earnings in period t
NPV	net present value
PU_{jpt}	purchases of product p made by plant j in period t
Q_{jkpt}^{PL}	flow of product p sent from plant j to warehouse k in period t
Q_{klpt}^{WH}	flow of product p sent from warehouse k to market l in period t
SA_{lpt}	sales of product p at market l in time period t
W_{ijpt}	input/output flow of product p associated with technology i at plant j in t
X_{ijt}^{PL}	binary variable (1 if the capacity of manufacturing technology i at plant j is expanded in time period t, 0 otherwise)
X_{kt}^{WH}	binary variable (1 if the capacity of warehouse k is expanded in time period t, 0 otherwise)
Y_{jkt}^{PL}	binary variable (1 if a transportation link between plant j and warehouse k is established in time period t, 0 otherwise)
Y_{klt}^{WH}	binary variable (1 if a transportation link between warehouse k and market l is established in time period t, 0 otherwise)

Acknowledgements

Gonzalo Guillén-Gosálbez expresses his gratitude for the financial support received from the Fulbright/Spanish Ministry of Education and Science visiting scholar program.

Appendix

For convenience in the presentation of the proofs, we set $f_d(x,y) = \ln \Phi(\frac{A_d}{B_d})$.

Proof of Proposition 1. Assume that $(\hat{x}, \hat{y})$ does not belong to the Pareto set of (P5). Then there is a solution of (P5) (x^*, y^*) that dominates $(\hat{x}, \hat{y})$, such that $f_d(x^*, y^*) > f_d(\hat{x}, \hat{y})$ for $d = 1, ..., D$. Since (P4) and (P5) have the same feasible region, then (x^*, y^*) is also feasible for (P4), and satisfies that $(\sum_d f_d(x^*, y^*)) > (\sum_d f_d(\hat{x}, \hat{y}))$. This contradicts the assumption that $(\hat{x}, \hat{y})$ is a global optimal solution of (P4). ■

Proof of Proposition 2. We first show that the function $\ln \Phi(\frac{p^t z}{q^t z})$, where p,q and z are two-dimensional vectors defined as follows $p^t = (1, 0)$, $q^t = (0, 1)$ and $z^t = (z^1, z^2)$, is pseudoconcave for $p^t z \geq 0$ and $q^t z \neq 0$ over a convex set S. Assume that z_1 and $z_2 \in S$, with $(z_2 - z_1)^t \nabla(\ln \Phi(\frac{p^t z_1}{q^t z_1})) \leq 0$. We need to show that $\ln \Phi(\frac{p^t z_2}{q^t z_2}) \leq \ln \Phi(\frac{p^t z_1}{q^t z_1})$. Note that:

$$\nabla \left(\ln \Phi \left(\frac{p^t z_1}{q^t z_1} \right) \right) = \frac{\frac{1}{\sqrt{2\pi}} e^{\frac{-1}{2}\left(\frac{p^t z_1}{q^t z_1}\right)^2}}{\Phi\left(\frac{p^t z_1}{q^t z_1}\right)} \left[\frac{(q^t z_1)\, p - (p^t z_1)\, q}{(q^t z_1)^2} \right] \tag{43}$$

Since $(z_2 - z_1)^t \nabla(\ln \Phi(\frac{p^t z_1}{q^t z_1})) \leq 0$ and since $\frac{\frac{1}{\sqrt{2\pi}} e^{\frac{-1}{2}\left(\frac{p^t z_1}{q^t z_1}\right)^2}}{\Phi\left(\frac{p^t z_1}{q^t z_1}\right)(q^t z_1)^2} \geq 0$, it follows that

$$(z_2 - z_1)^t \left[\left(q^t z_1\right) p - \left(p^t z_1\right) q \right] \leq 0 \tag{44}$$

which leads to

$$0 \geq \left(z_2^1 - z_1^1, z_2^2 - z_1^2\right) \begin{pmatrix} z_1^2 \\ -z_1^1 \end{pmatrix} = \left(z_2^1 - z_1^1\right)\left(z_1^2\right) - \left(z_2^2 - z_1^2\right)\left(z_1^1\right) = \left(z_2^1 z_1^2 - z_2^2 z_1^1\right) \tag{45}$$

This implies that $\frac{z_2^1}{z_2^2} \leq \frac{z_1^1}{z_1^2}$, which in turn leads to $\ln \Phi(\frac{p^t z_2}{q^t z_2}) \leq \ln \Phi(\frac{p^t z_1}{q^t z_1})$, since $\ln \Phi(\cdot)$ is monotone increasing. Therefore, $\ln \Phi(\frac{A_d}{B_d})$ is pseudoconcave. From Theorem 3.5.11 in Bazaraa et al. (1979), $\ln \Phi(\frac{A_d}{B_d})$ is also quasiconcave and strictly quasiconcave. Thus, (P6) is a maximization problem with a pseudoconcave objective function subject to a set of linear equality constraints and convex and quasiconvex inequality constraints (i.e., all the original constraints of (P5) are linear except one that is nonlinear but convex, and the epsilon constraints of the form $\epsilon_d - \ln \Phi(\frac{A_d}{B_d}) \leq 0$ have been shown to be quasiconvex). Then, from Theorem 4.3.8 in Bazaraa et al. (1979), a point satisfying the

KKT conditions for such a problem is also a global maximum over the feasible region, and the proof is complete. ■

Proof of Proposition 3. Consider the Karush-Kuhn-Tucker conditions of problem (P4) that are satisfied in $(\hat{x}, \hat{y})$:

$$\sum_{d \in D} \nabla f_d(\hat{x}, \hat{y}) + \sum_{l \in A_l} \overline{u_l} \nabla g_l(\hat{x}, \hat{y}) + \sum_{j \in J} \overline{v_j} \nabla h_j(\hat{x}, \hat{y}) = 0 \tag{46}$$

where $A_l := \{l : g_l(x) = 0\}$, and $\overline{u_l}$ for $l \in A_l$, and $\overline{v_j}$ for $j = 1, ..., J$, denote the Karush-Kuhn-Tucker multipliers for the active inequality and equality constraints, respectively. Now consider the KKT conditions of (P6):

$$\nabla f_k(x, y) - \sum_{d \neq k} \overline{u_d} \nabla f_d(x, y) + \sum_{l \in A_l} \overline{u_l} \nabla g_l(x, y) + \sum_{j \in J} \overline{v_j} \nabla h_j(x, y) = 0 \tag{47}$$

where $\overline{u_d}$ are the Lagrangean multipliers associated with the epsilon constraints (i.e., $\epsilon_d - \ln \Phi(\frac{A_d}{B_d}) \leq 0$), which are mathematically given by:

$$\overline{u_d} = \left(\frac{\partial f_k(x, y)}{\partial f_d(x, y)} \right)_{(\delta f_i(x,y)=0,\, i \neq d,k) \wedge (\delta g_l(x,y)=0)} \qquad d \neq k$$

If we substitute $(\hat{x}, \hat{y})$ in 47 and set $\overline{u_d} = -1$, then this solution satisfies the KKT conditions of (P6). Notice that by imposing the condition $\overline{u_d} = -1$, the point also satisfies equation 40. Furthermore, from Proposition 2, we know that a KKT point of (P6) is a global maximum of (P6). Finally, from Proposition 4.1 in Ehrgott (2000) we know that a global optimal solution of (P6) is a Pareto solution of (P5), and the proof is complete. ■

Proof of Proposition 4. Assume that $(\hat{x}, \hat{y})$ is a feasible solution of (P7) that satisfies $(\sum_d f_d(\hat{x}, \hat{y})) > \left(UB_k^i + \sum_{d \neq k} \overline{\epsilon_d^i}\right)$. This implies that there exists at least one term of the summation on the left hand side of the inequality with a higher value than its counterpart on the right hand side. First, assume that $f_d(\hat{x}, \hat{y}) > \overline{\epsilon_d^i}$ for at least one $d \neq k$. This contradicts the assumption that $(\hat{x}, \hat{y})$ is a feasible solution of (P7). Second, assume that $f_k(\hat{x}, \hat{y}) > UB_k^i$. Since the feasible region of (P7) is tighter than that of (P8), a global maximum of (P8) yields a valid upper bound on the value of $f_k(\hat{x}, \hat{y})$ over the feasible region of (P7). This contradicts $f_k(\hat{x}, \hat{y}) > UB_k^i$, and the proof is complete. ■

References

Bazaraa, M. S., Sherali, H. D., Shetty, C. M., 1979. Nonlinear programming, theory and algorithms. John Wiley & Sons, Inc.

Brooke, A., Kendrik, D., Meeraus, A., Raman, R., Rosenthal, R. E., 1998. GAMS - A User's Guide. GAMS Development Corporation, Washington.

Ehrgott, M., 2000. Multicriteria optimization. Springer.

Guillén-Gosálbez, G., Grossmann, I., 2008. Optimal design and planning of sustainable chemical supply chains under uncertainty. Submitted to AIChE Journal .

Haimes, Y. Y., Lasdon, L. S., Wismer, D. A., 1971. On a bicriterion formulation of the problems of integrated system identification and system optimization. IEEE Transactions on Systems, Man and Cybernetics 1, 296–297.

Heijungs, R., Frischknecht, R., 2005. Representing statistical distributions for uncertain parameters in lca. Int J LCA 10(4), 248–254.

Heijungs, R., Suh, S., Kleijn, R., 2005. Numerical approaches to life cycle interpretation. Int J LCA 10(2), 103–112.

Kataoka, S., 1963. A stochastic programming model. Econometrica 31(1-2), 181–196.

PRé-Consultants, 1998. SimaPro 6 LCA software. The Netherlands (www.pre.nl/simapro/default.htm).

PRé-Consultants, 2000. The eco-indicator 99, a damage oriented method for life cycle impact assessment. methodology report and manual for designers. Tech. rep., PRé Consultants, Amersfoort, The Netherlands.

Sugiyama, H., Fukushima, Y., Hirao, M., Hellweg, S., Hungerbühler, K., 2005. Using standard statistics to consider uncertainty in industry-based life cycle inventory databases. Int J LCA 10(6), 339–405.

Captions for Figures

List of Figures

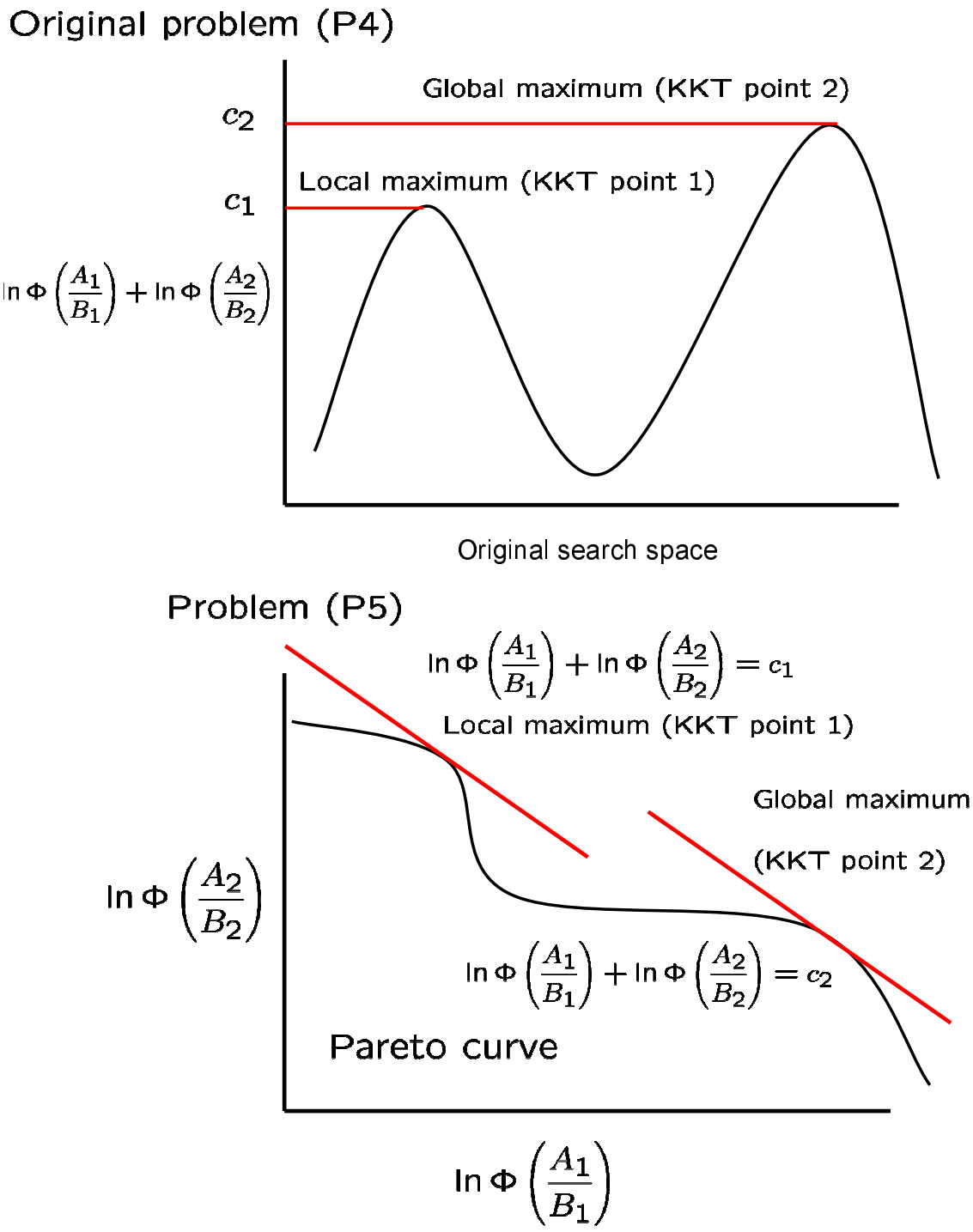

Fig. 1. Illustrative example of Propositions 1 and 2.

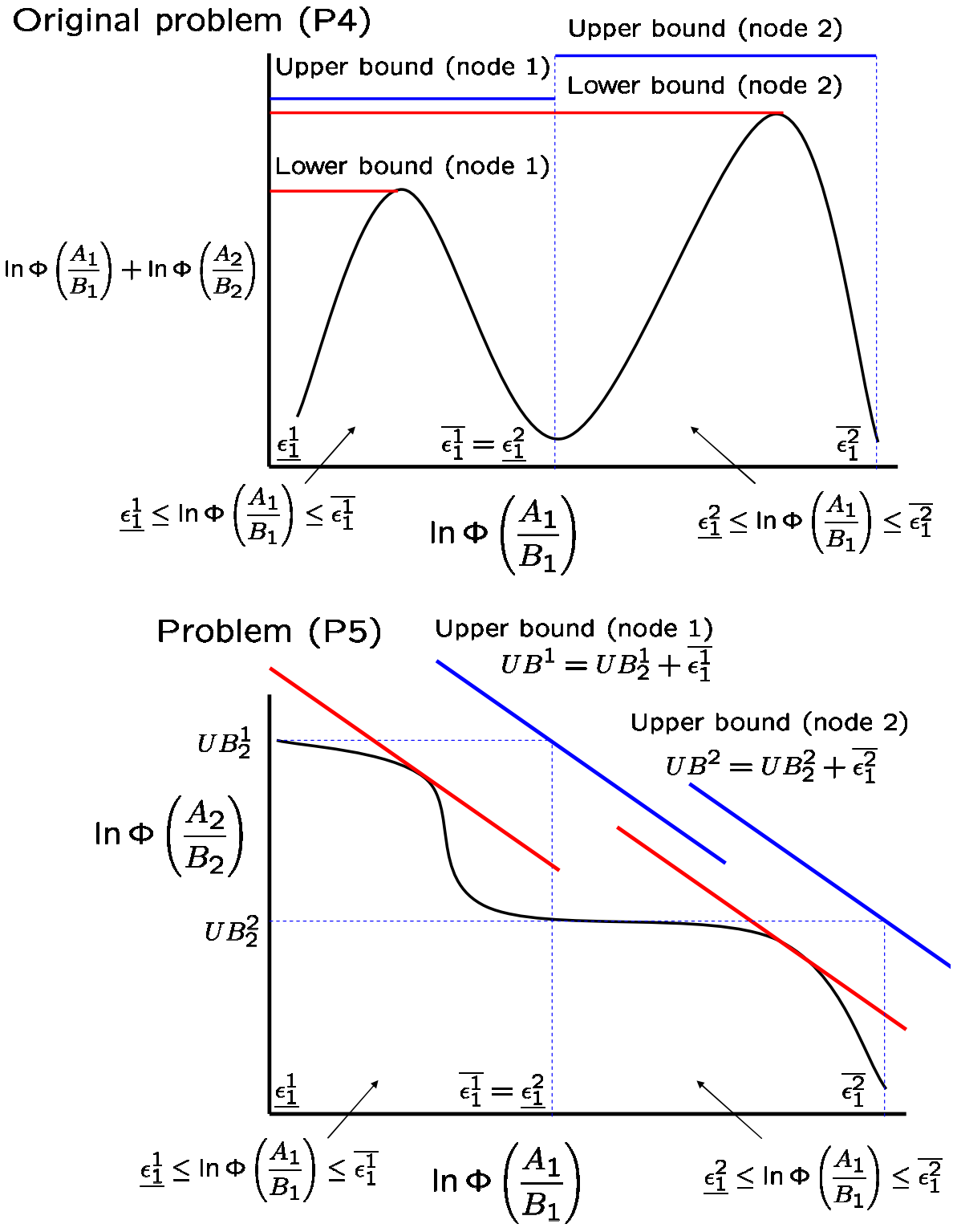

Fig. 2. Spatial branch and bound.

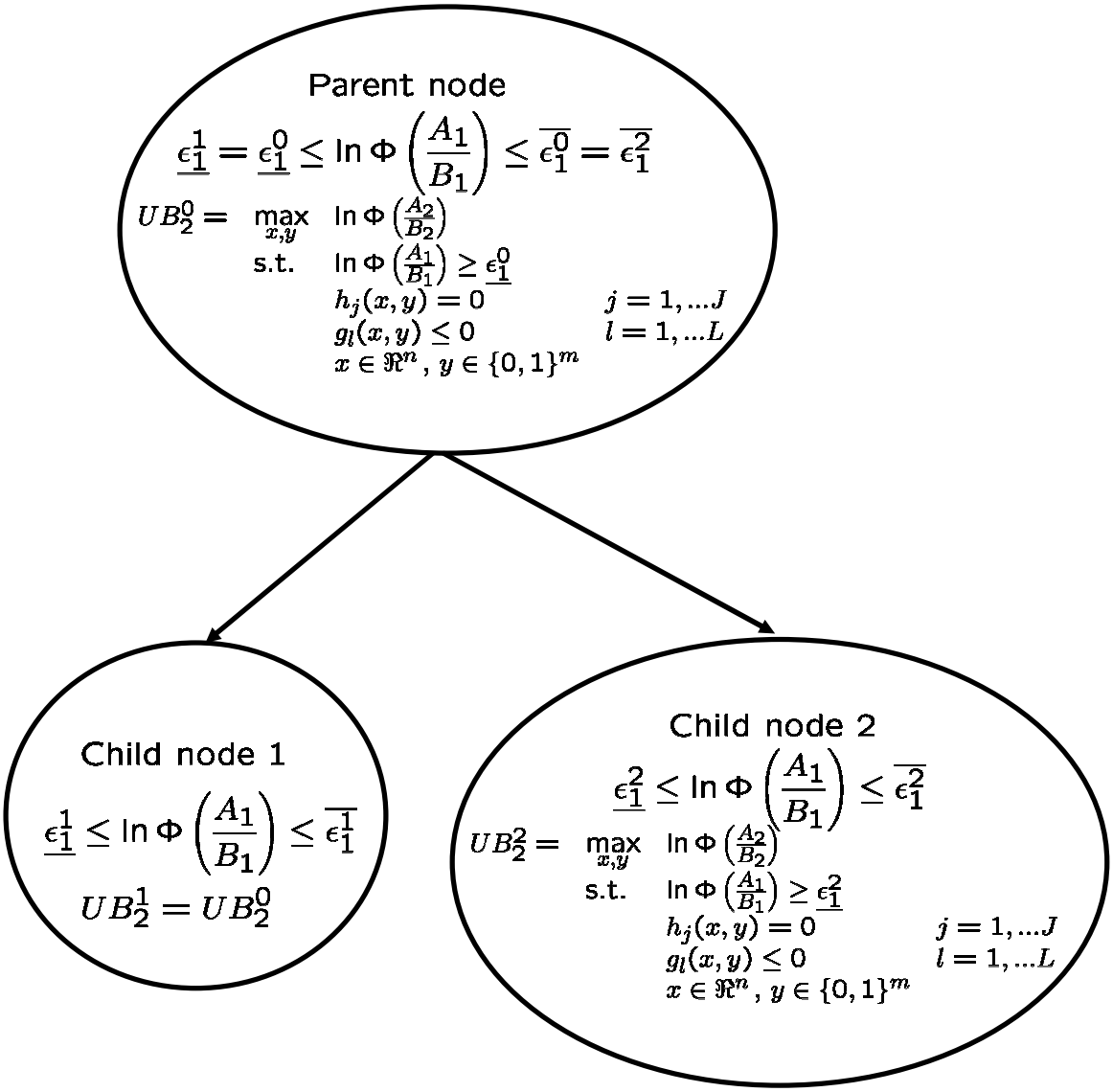

Fig. 3. Spatial branch and bound.

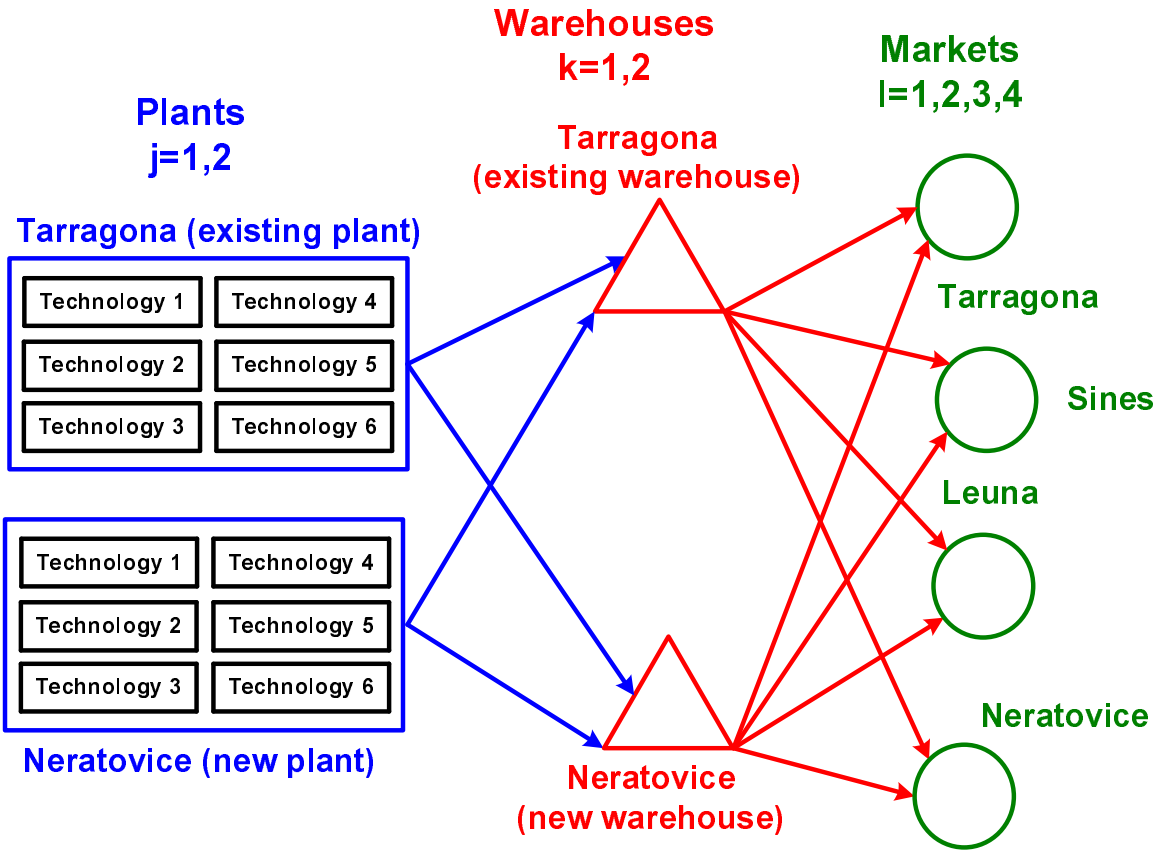

Fig. 4. Case study.

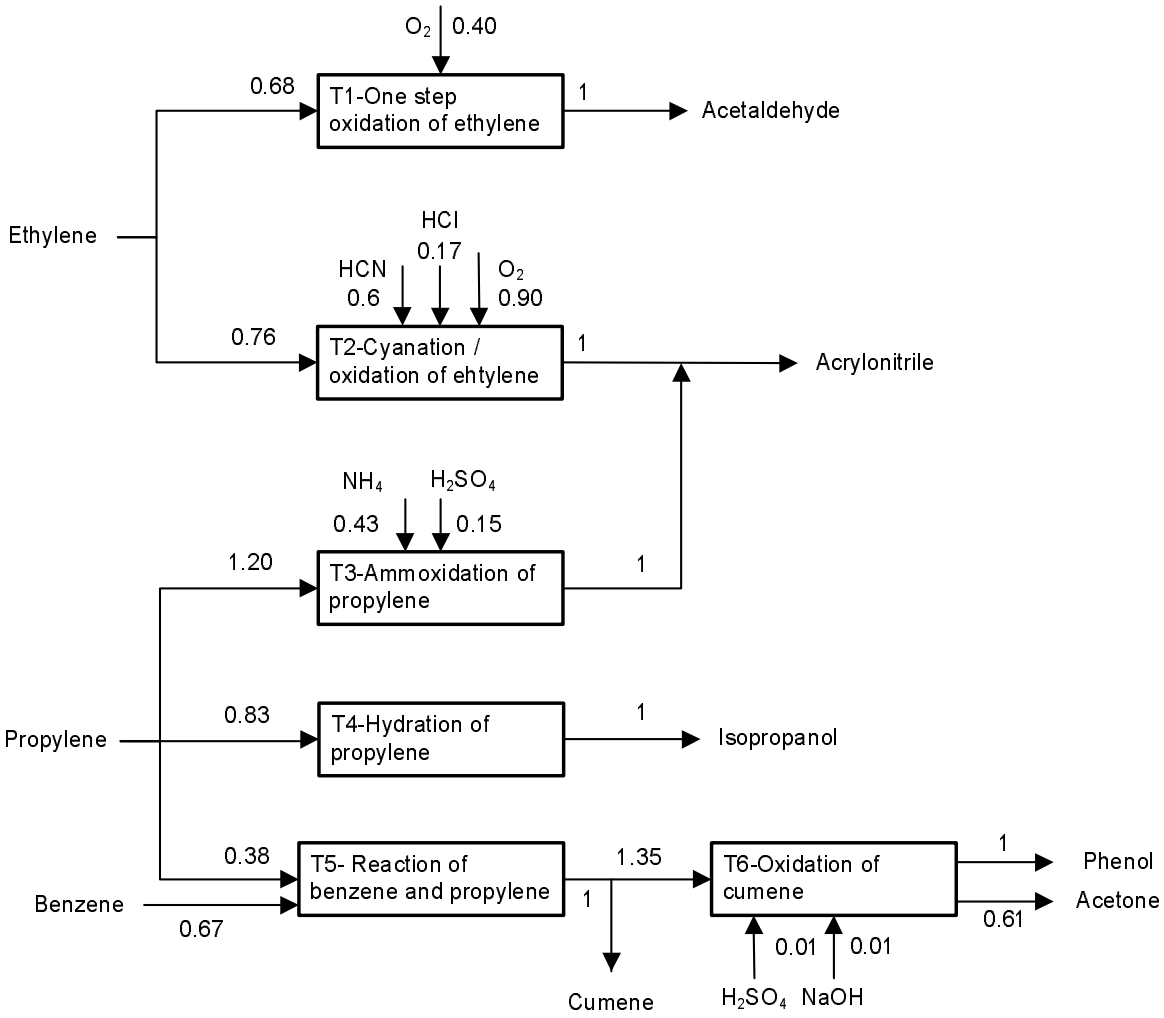

Fig. 5. Superstructure of technologies.

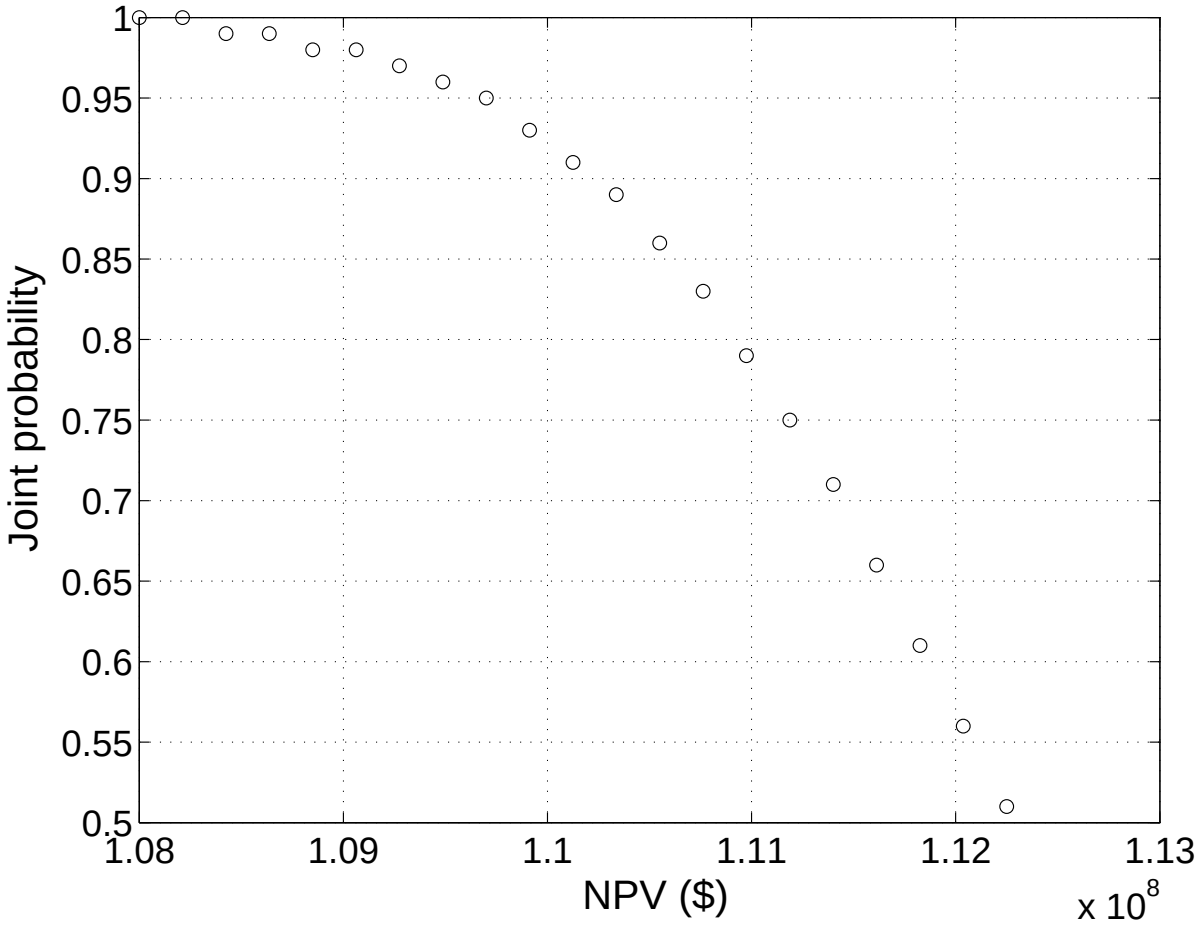

Fig. 6. Pareto set of case study 1a.

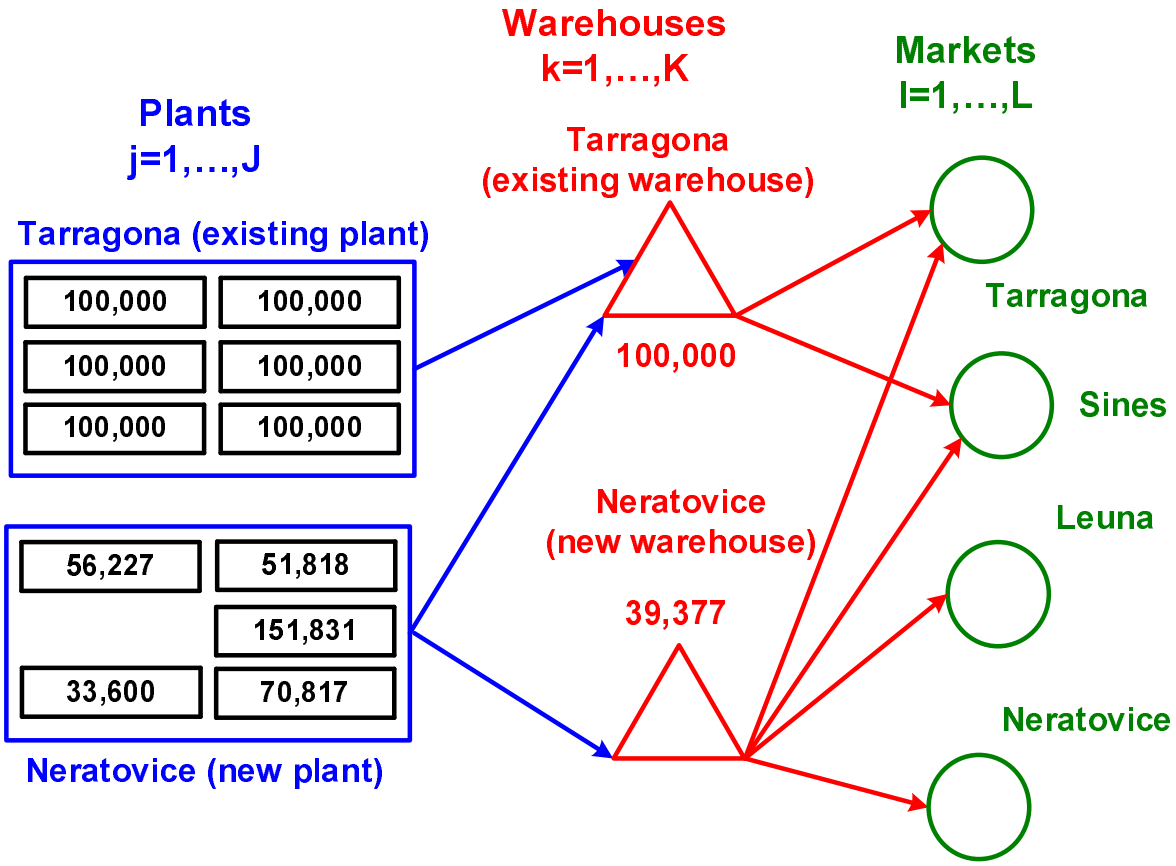

Fig. 7. Maximum NPV solution.

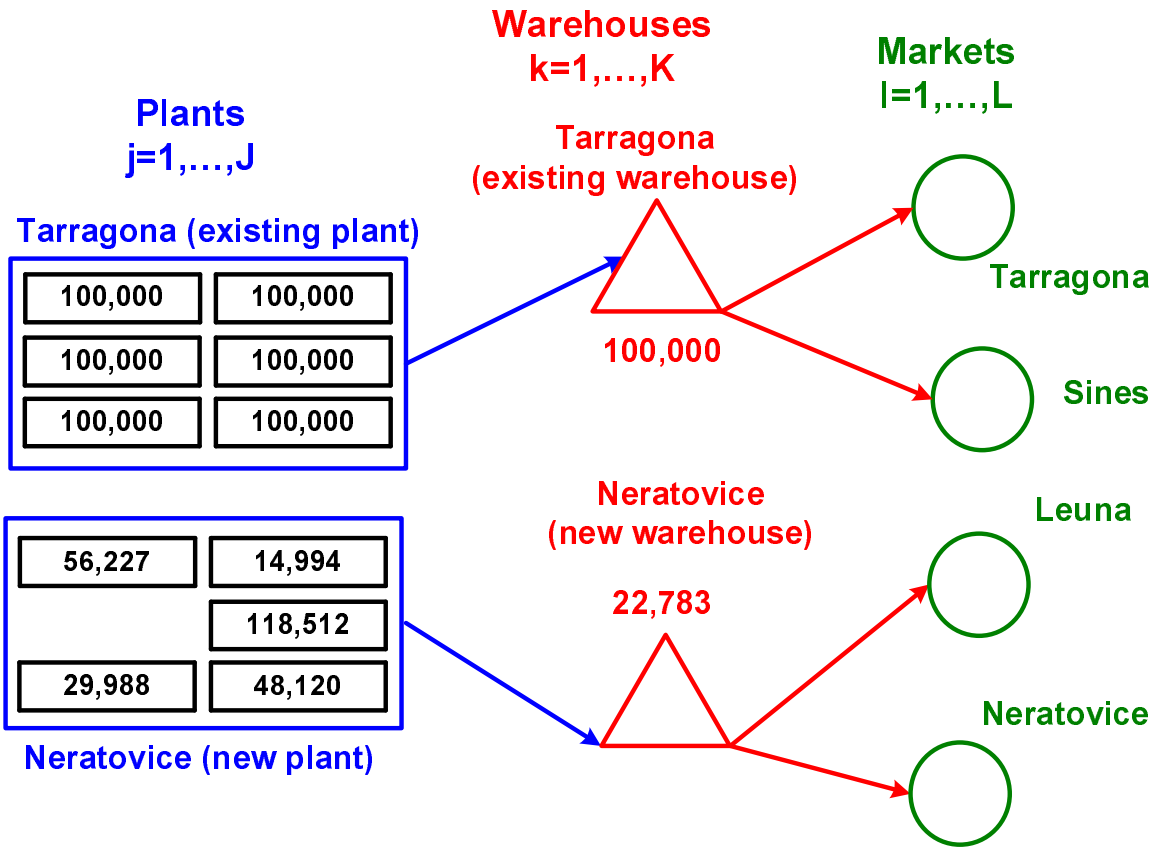

Fig. 8. Minimum environmental impact solution.

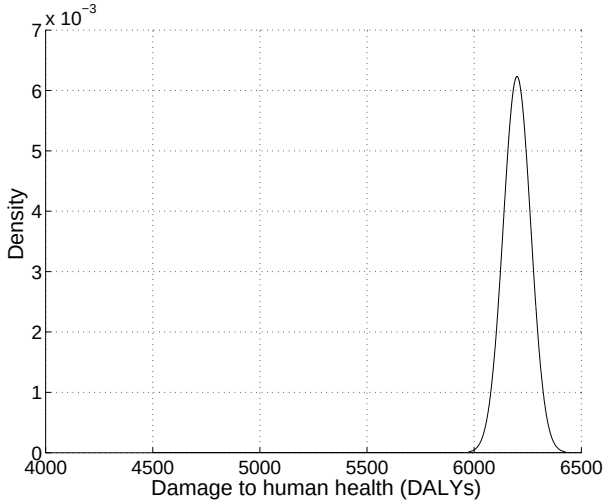

(a) Maximum NPV

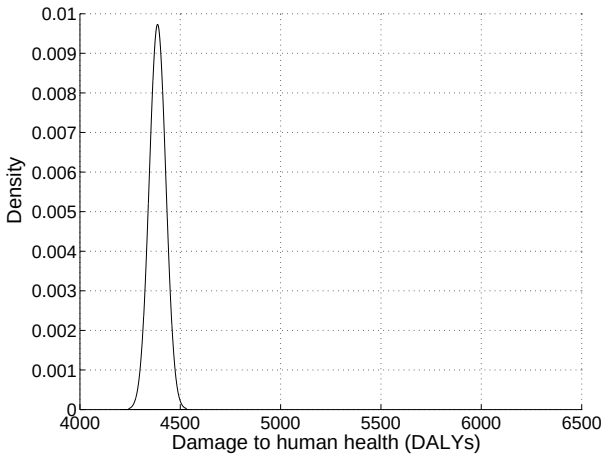

(b) Minimum environmental impact

Fig. 9. Probability curves (impact category: human health)

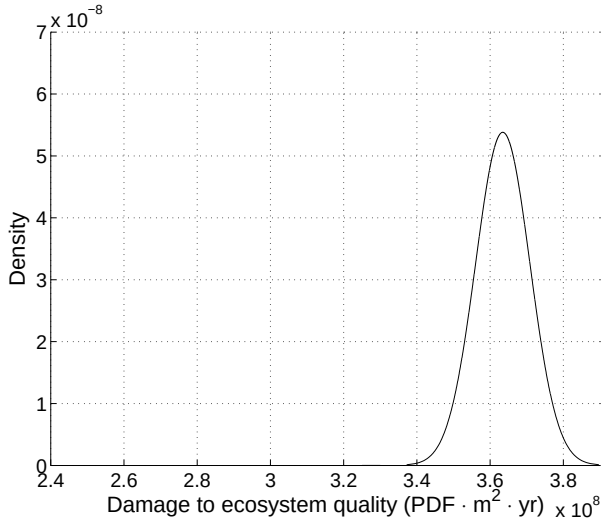

(a) Maximum NPV

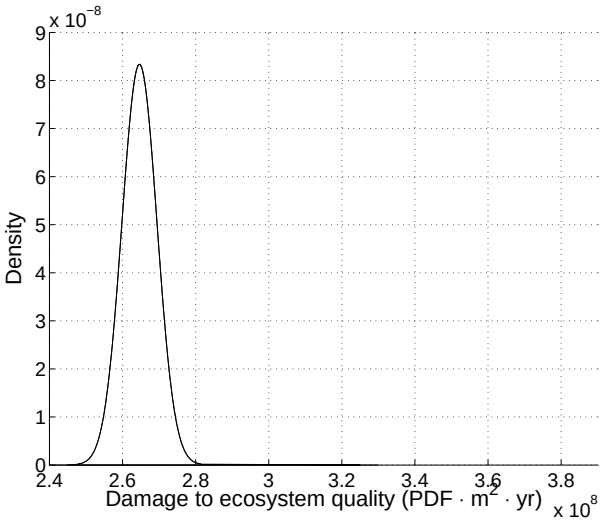

(b) Minimum environmental impact

Fig. 10. Probability curves (impact category: ecosystem quality)

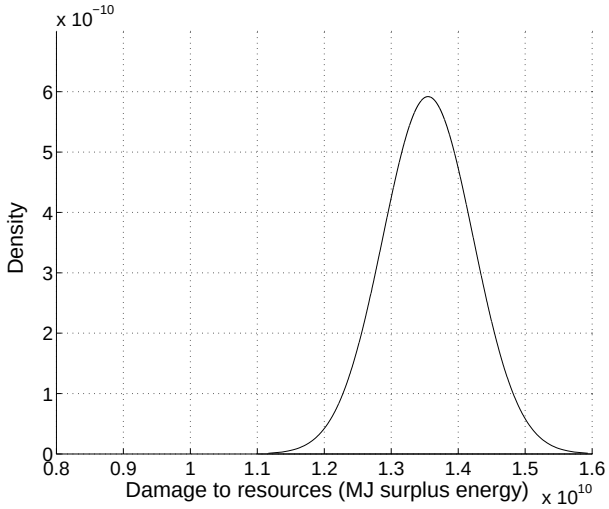

(a) Maximum NPV

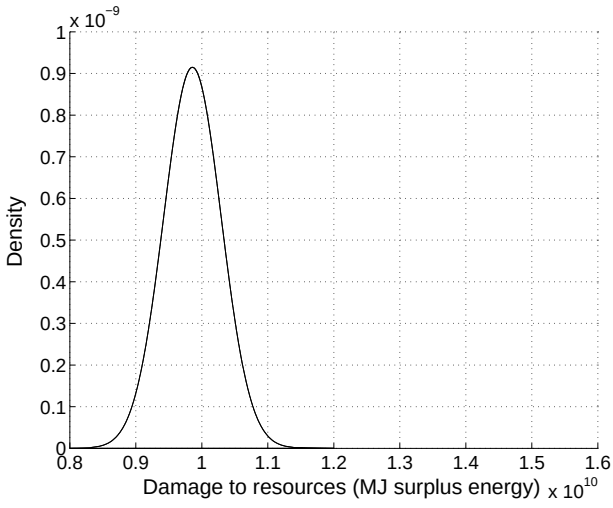

(b) Minimum environmental impact

Fig. 11. Probability curves (impact category: resources)

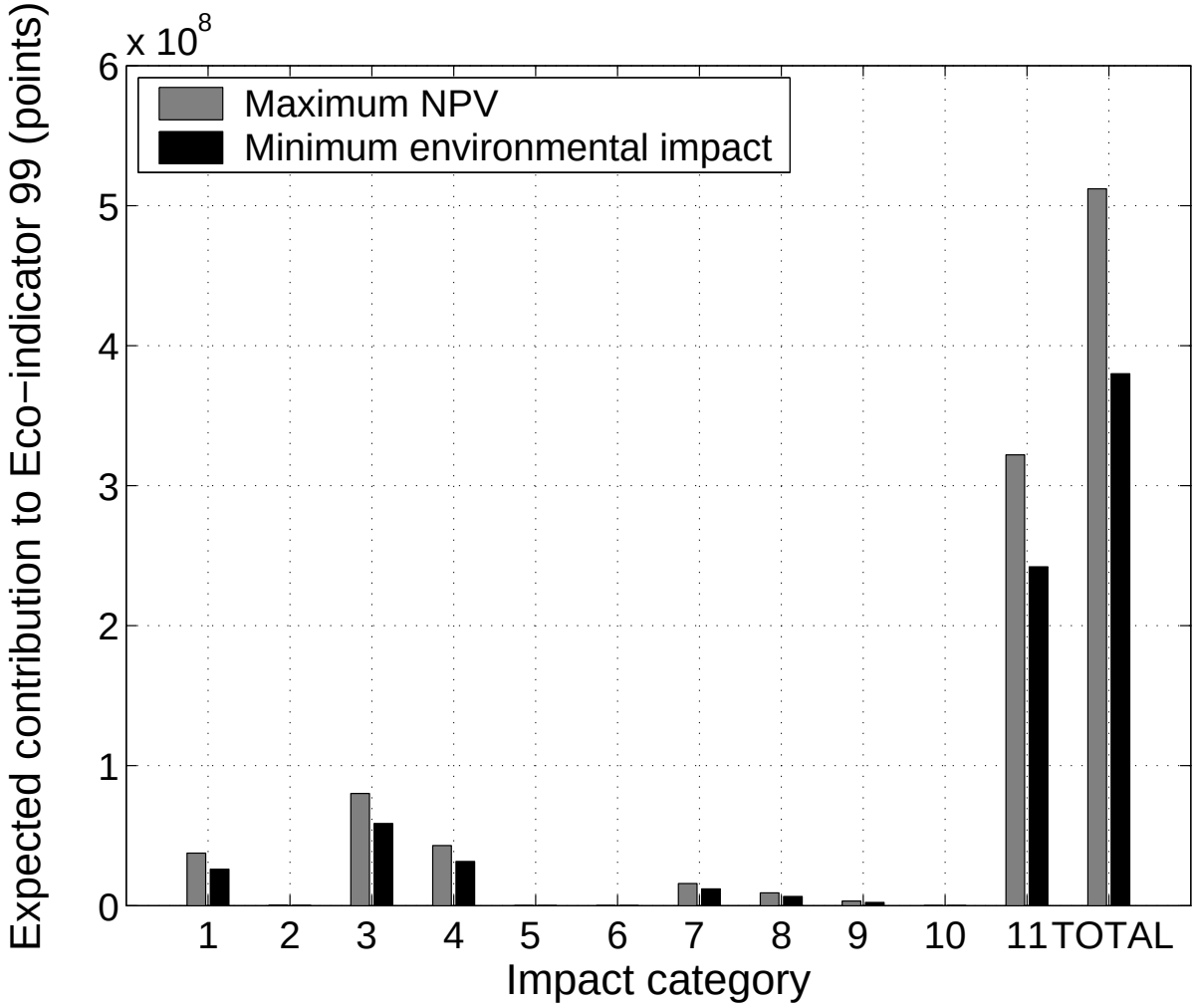

Fig. 12. Impact categories of Eco-indicator 99.

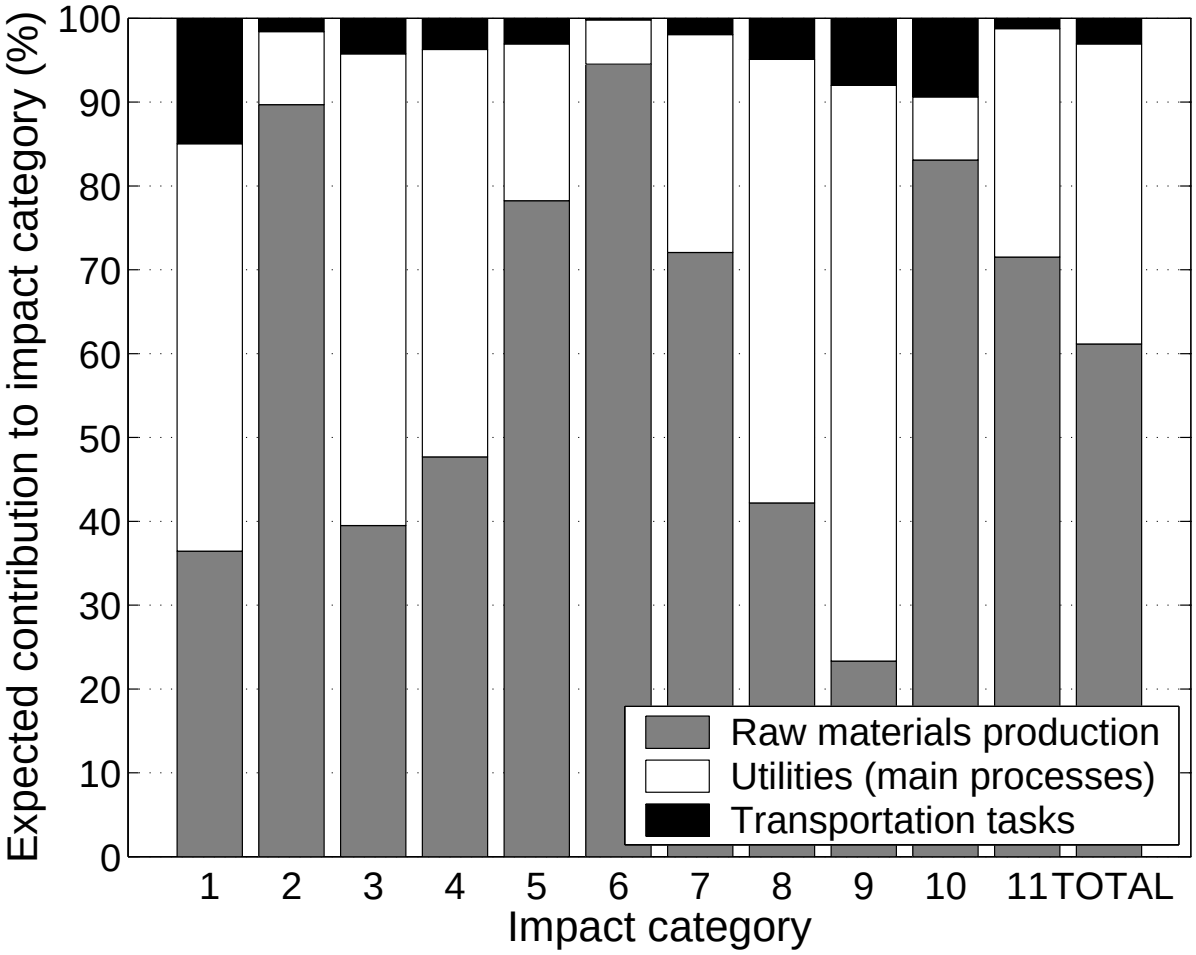

Fig. 13. Expected contribution to Eco-indicator 99 (maximum NPV solution).

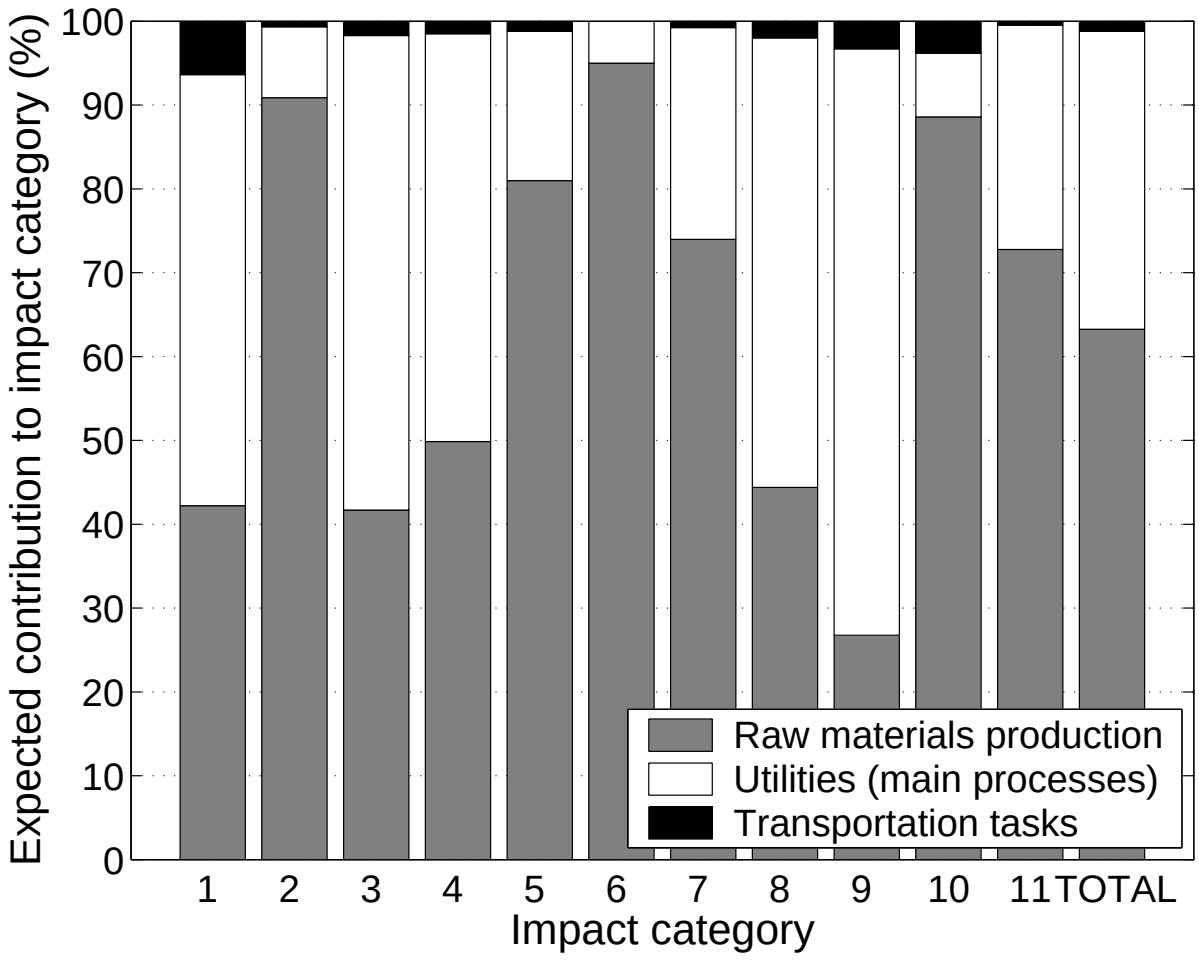

Fig. 14. Expected contribution to Eco-indicator 99 (minimum environmental impact solution).

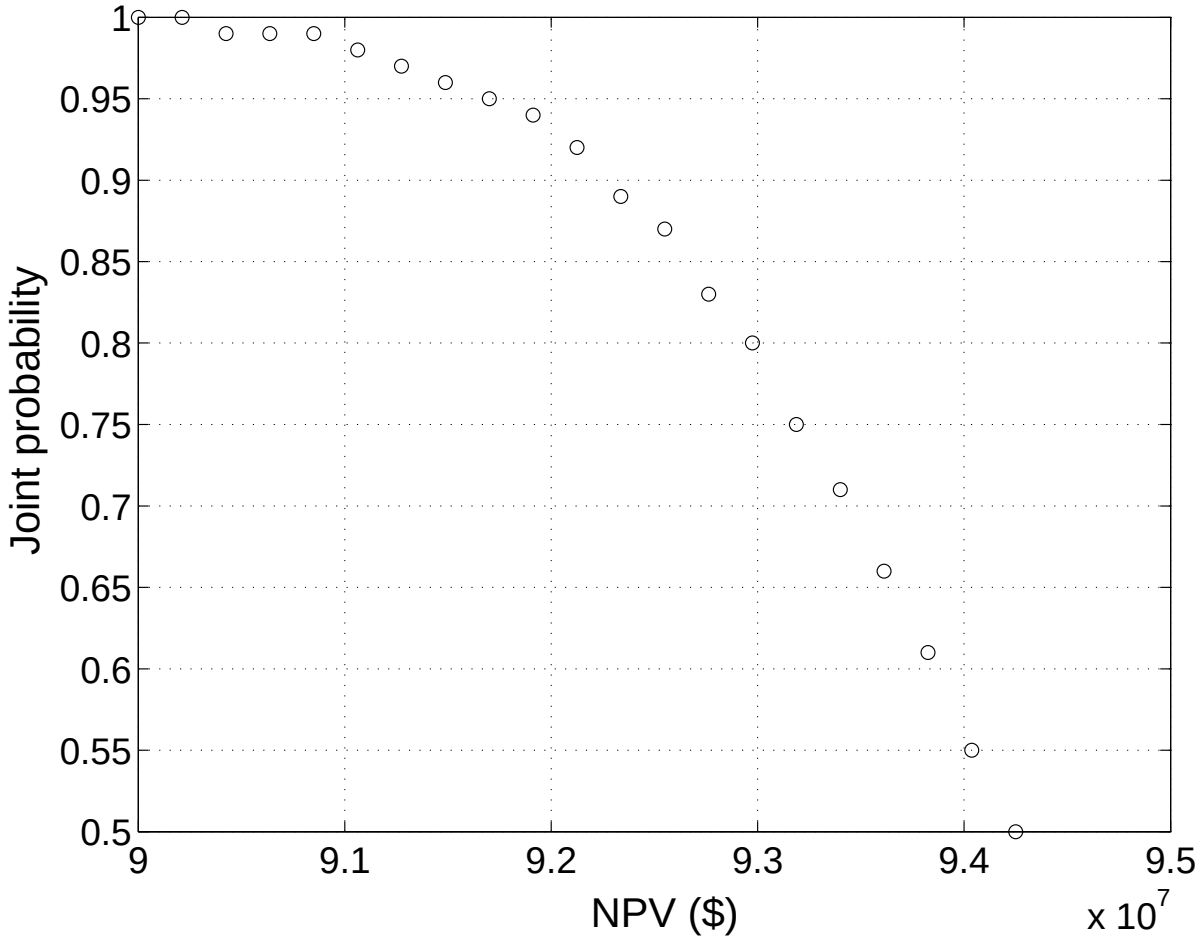

Fig. 15. Pareto set of case study 1b.

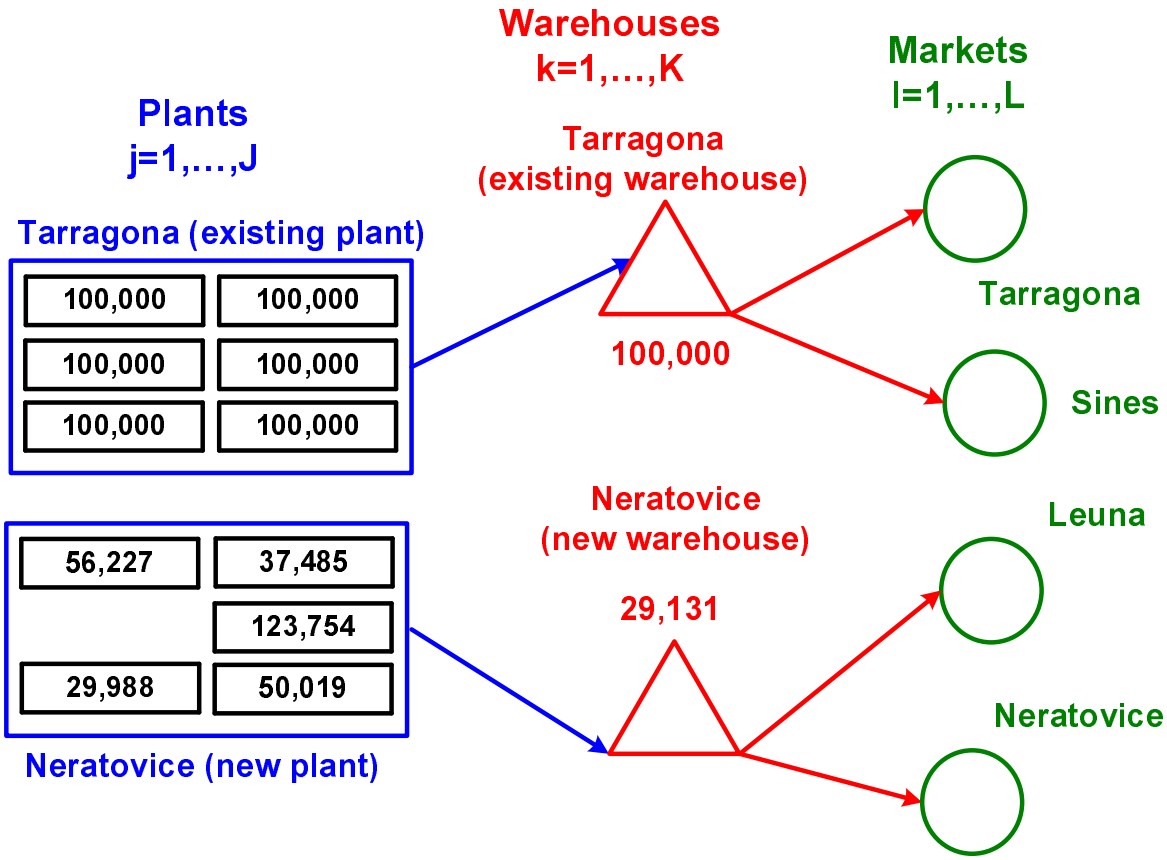

Fig. 16. Maximum NPV solution.

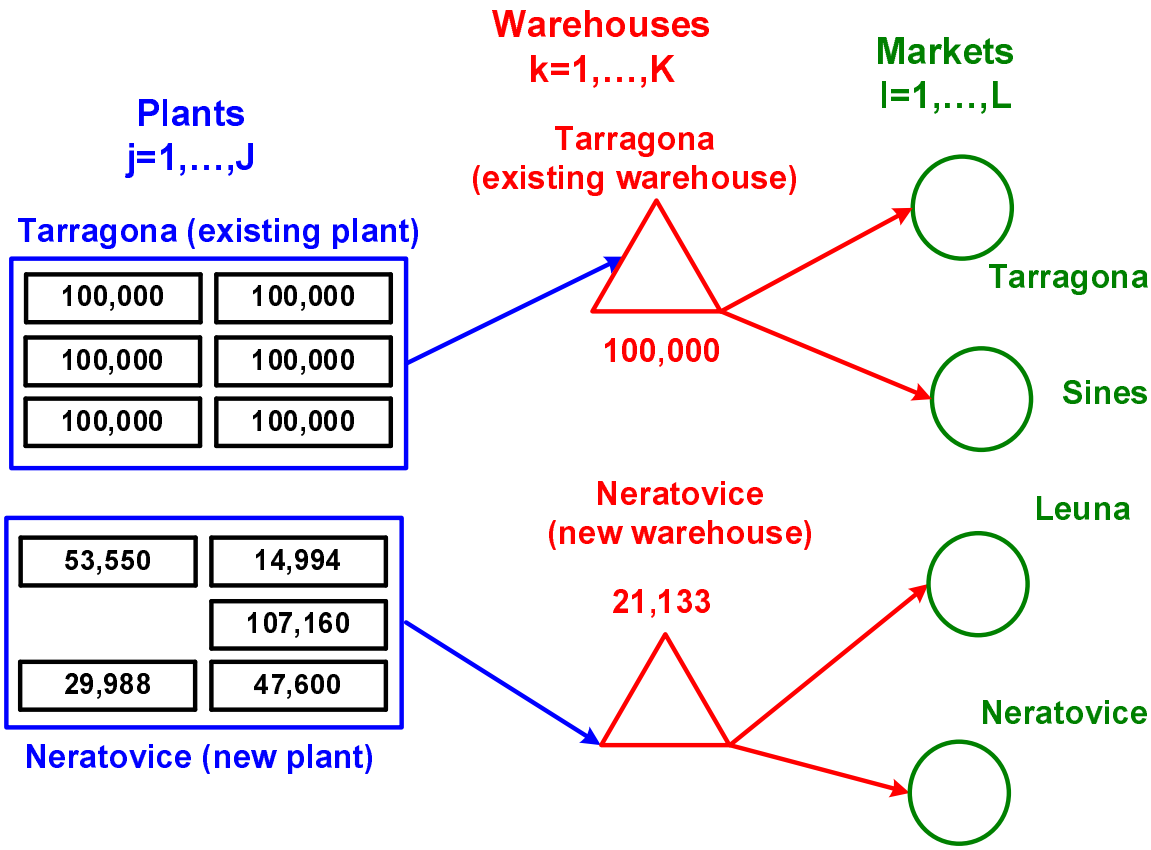

Fig. 17. Minimum environmental impact solution.

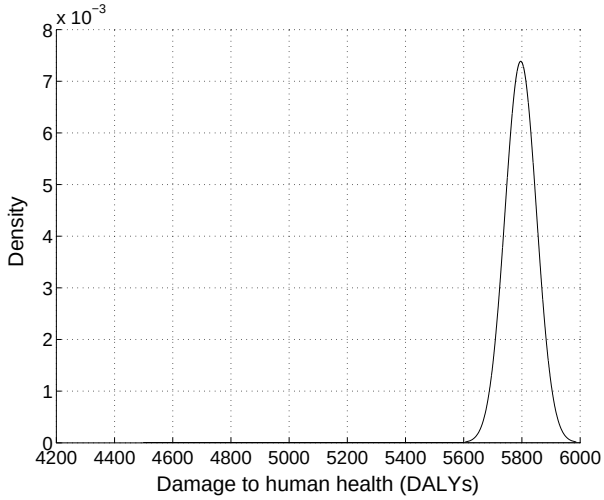

(a) Maximum NPV

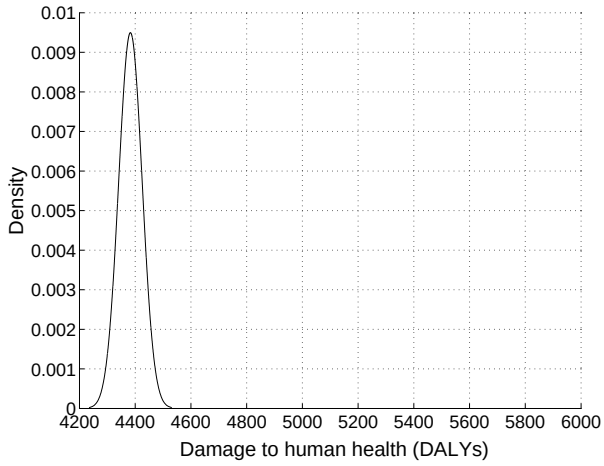

(b) Minimum environmental impact

Fig. 18. Probability curves (impact category: human health)

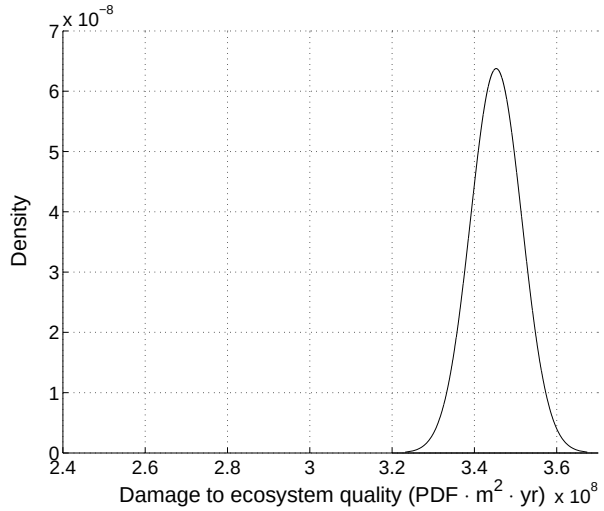

(a) Maximum NPV

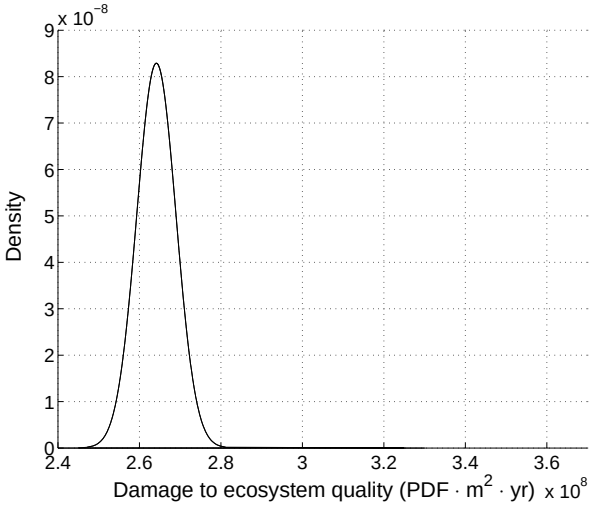

(b) Minimum environmental impact

Fig. 19. Probability curves (impact category: ecosystem quality)

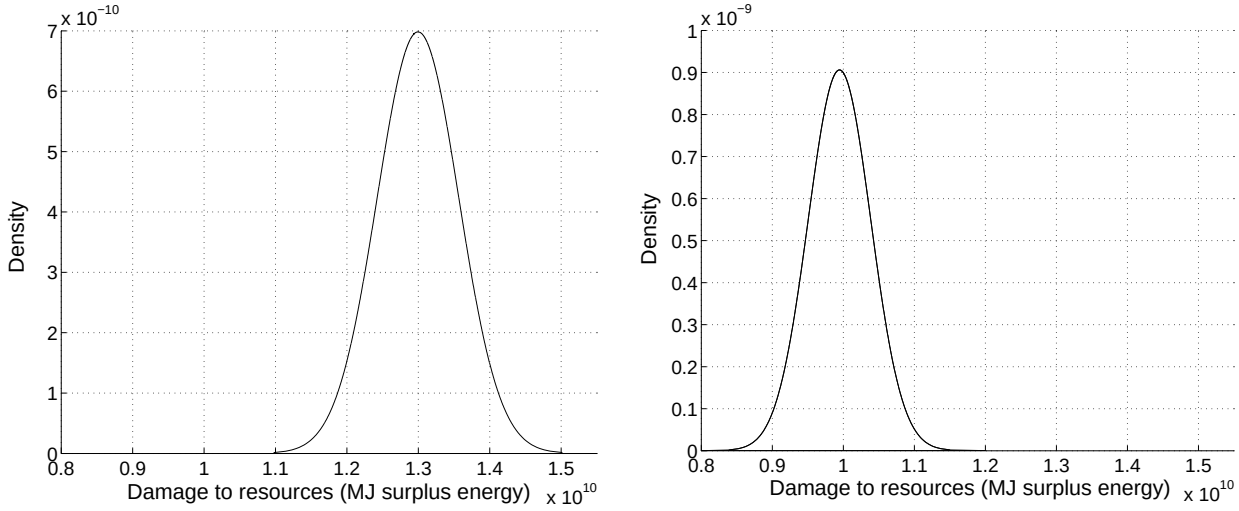

(a) Maximum NPV

(b) Minimum environmental impact

Fig. 20. Probability curves (impact category: resources)

Headings of Tables

List of Tables

Table 1
Case study 1: variable and fixed investment cost of plants for $t = 1$ (assume a 5% increase in each period of time)

	α_{ijt}^{PL} (\$/ton)		β_{ijt}^{PL} (thousand \$)	
Tech./Plant	Neratovice	Tarragona	Neratovice	Tarragona
T1	48.68	91.28	4,430.11	8,306.45
T2	49.83	93.43	4,534.83	8,502.82
T3	125.76	235.81	11,445.06	21,459.49
T4	55.86	104.73	5,083.10	9,530.80
T5	24.71	46.34	2,248.92	4,216.72
T6	88.31	165.59	8,036.80	15,069.01

Table 2
Case study 1: operating cost for $t = 1$ (assume a 5% increase in each period of time) and consumption of energy

	υ_{ijpt} (\$/ton)		η_{ijp}^{EN}
Tech./Plant	Neratovice	Tarragona	(FOET/ton)
T1	7.12	16.03	0.22
T2	19.43	43.71	0.60
T3	4.86	10.93	0.15
T4	12.30	27.68	0.38
T5	1.94	4.37	0.06
T6	12.30	27.68	0.38

Table 3
Case study 1: price of final products for $t = 1$ (assume a 5% increase in each period of time)

	γ_{lpt}^{FP} (\$/ton)			
Chemical/Market	Leuna	Neratovice	Sines	Tarragona
acetaldehyde	509.26	487.43	491.07	500.17
acetone	432.87	414.32	417.41	425.14
acrylonitrile	36.40	34.84	35.10	35.75
cumene	401.23	384.04	386.90	394.07
isopropanol	401.23	384.04	386.90	394.07
phenol	709.88	679.45	684.52	697.20

Table 4
Case study 1: cost of raw materials for $t = 1$ (assume a 5% increase in each period of time)

	γ_{jpt}^{RM} (\$/ton)	
Chemical/Plant	Neratovice	Tarragona
ammonia	140.54	148.81
benzene	200.51	212.30
ethylene	233.68	247.42
hydrochloric acid	116.18	123.02
hydrogen cyanide	468.47	496.03
oxygen	29.98	31.75
propylene	159.28	168.65
sodium hidroxide	140.54	148.81
sulfuric acid	42.16	44.64

Table 5
Case study 1: demand of products for $t = 1$ (assume a 5% increase in each period of time)

	$\overline{D_{lpt}^{MK}}$ (kton/year)			
Chemical/Market	Leuna	Neratovice	Sines	Tarragona
acetaldehyde	13.5	37.5	12.0	7.5
acetone	10.8	30.0	9.6	6.0
acrylonitrile	18.0	50.0	16.0	10.0
cumene	13.5	37.5	12.0	7.5
isopropanol	9.0	25.0	8.0	5.0
phenol	12.6	35.0	11.2	7.0

Table 6
Case study 1: matrix of distances

	λ_{kl}^{WH} (km)			
Ware./Market	Leuna	Neratovice	Sines	Tarragona
Neratovice	295.45	0	2,970.72	1,855.47
Tarragona	1,781.36	1,855.47	1,212.82	0

Table 7
Case study 1: variable and fixed investment cost and operating cost of warehouses for $t = 1$ (assume a 5% increase in each period of time)

Warehouse	α_{kt}^{WH} (\$/ton)	β_{kt}^{WH} (thousand \$)	π_{kt} (\$/ton)
Neratovice	1.06	96.31	0.10
Tarragona	2.38	216.69	0.22